# Controls on barium incorporation into tests of benthic foraminifera from the Aegean Sea (Eastern Mediterranean Sea) – Towards a species-specific Ba/Ca calibration

Jassin Petersen [a,*] , Gerhard Schmiedl [b], Jacek Raddatz [c,d,1], André Bahr [e], Jörg Pross [e], Meryem Mojtahid [f]

[a] Institute of Geology and Mineralogy, University of Cologne, Otto-Fischer-Straße 14, 50674 Cologne, Germany
[b] Center for Earth System Sciences and Sustainability, Institute for Geology, University of Hamburg, Bundesstraße 55, 20146 Hamburg, Germany
[c] Institute of Geosciences, Goethe University Frankfurt, Altenhöferallee 1, 60438 Frankfurt am Main, Germany
[d] Frankfurt Isotope and Element Research Center (FIERCE), Goethe University Frankfurt, 60438 Frankfurt, Germany
[e] Institute of Earth Sciences, Heidelberg University, Im Neuenheimer Feld 234, 69120 Heidelberg, Germany
[f] Université d'Angers, Université de Nantes, Université Le Mans, CNRS, LPG, UMR 6112, 2 Bd Lavoisier, 49045 Angers Cedex, France

## ARTICLE INFO

## ABSTRACT

We have analysed Ba/Ca ratios of live and dead benthic foraminifera (*Uvigerina mediterranea* and *Melonis affinis*) from core tops of seven sites located in the Aegean Sea by laser ablation ICP-MS. There are no significant Ba/Ca differences in live and dead specimens of *U. mediterranea*. For *M. affinis* we apply a threshold criterion for extremely high Ba/Ca in live specimens in order to highlight the overall uniform Ba/Ca signal. The Ba/Ca intra-test variability varies between 16 and 24 % relative standard deviation per specimen. It is attributed to bio-mineralisation processes i.e., vital effects. The Ba/Ca ratios of *M. affinis* are significantly higher than those of *U. mediterranea* throughout most of the sites and their respective samples from different sediment depths. The influence on Ba/Ca of both species by biomineralisation processes and/or microhabitat effects remains open. Linking the Ba/Ca ratios to measured Ba concentration of bottom waters from one of the studied sites, shows partition coefficients of $D_{Ba} = 0.34$, and $D_{Ba} = 0.49$ for *U. mediterranea* and *M. affinis*, respectively. We could not identify trends of Ba/Ca ratios to observed/ modelled gradients of relevant environmental factors between the seven analysed sites, such as primary productivity and associated $C_{org}$ fluxes or TOC concentrations. Despite the demonstrated limited proxy potential in these parts of the Aegean Sea, we suggest that it is possible to employ Ba/Ca of infaunal benthic species in order to reconstruct export productivity in deep-sea areas with a less complex linkage between primary productivity and nutrient distribution in bottom waters.

## 1. Introduction

The processes controlling the marine carbon and barium cycles are closely coupled, therefore allowing the reconstruction of export productivity through the assessment of the Ba content in the geological record (Bishop, 1988; Paytan and Kastner, 1996; Carter et al., 2020). Models and global ocean data show that an export of organic matter (OM) from the upper ocean into the deep ocean is correlated to the flux of dissolved Ba from upper to deep oceans, and also to barite formation in the sediment (Dymond and Collier, 1996; Paytan and Kastner, 1996; Dickens et al., 2003). Some of these models show that to maintain such a scenario, an additional source of dissolved Ba to the upper water column of oceans is needed, i.e., riverine input (Paytan and Kastner, 1996; Carter et al., 2020). Historically, biogenic Ba fluxes normalized to [230]Th, as well as Ba/Th and Ba/Al ratios of sediment records have been used to link the Ba and carbon cycles and reconstruct export productivity (e.g., Dehairs et al., 2000; Moller et al., 2012; Jaccard et al., 2013). Generally, sedimentary signatures are subject to primary and secondary diagenetic alteration, and in the case of Ba, barite dissolution occurs when $SO_4^{2-}$ concentrations decrease below a threshold in surface sediments, and barite can (re)precipitate diagenetically (Church and Wolgemuth, 1972; McManus et al., 1998; Schenau et al., 2001). For organic-rich sediments

* Corresponding author.
  *E-mail address:* jassin.petersen@uni-koeln.de (J. Petersen).
  [1] present address: GEOMAR Helmholtz Centre for Ocean Research Kiel, Wischhofstr.1–3, 24,148 Kiel, Germany

such as sapropel layers from the Mediterranean Sea (Section 1.1), there is the phenomenon of a burndown effect, altering the geochemical composition of most recently deposited layers (Higgs et al., 1994; Thomson et al., 1995; Möbius et al., 2010). Regarding Ba, it was shown that post-depositional processes such as oxidation do not decrease its content in sapropelic sediments, underlining its potential as proxy for palaeo-export productivity (Thomson et al., 1995, 2006; Moller et al., 2012).

Benthic foraminifera colonize the surface sediment and precipitate their carbonate tests with an elemental and isotopic composition reflecting the surrounding bottom water and pore water composition, allowing for the reconstruction of palaeoenvironmental parameters (e. g., McCorkle et al., 1997; Schmiedl et al., 2004; Koho et al., 2015). The Ba/Ca ratios of fossil benthic foraminiferal tests may conserve the signal of $Ba^{2+}$ of the bottom and pore waters, from which the foraminifera have calcified their test, and which is thought to reflect the input of Ba and thus OM fluxes from the water column (e.g., Ní Fhlaithearta et al., 2010; Mojtahid et al., 2019). The further development of this proxy requires a profound understanding of the underlying processes for the incorporation of Ba in foraminiferal carbonate, partly stemming from calibration studies on core tops or undisturbed surface sediment samples, as well as culturing experiments in the laboratory. In fact, such calibration studies have been performed for Ba/Ca of benthic foraminifera from culturing experiments (Havach et al., 2001; de Nooijer et al., 2017) and core tops (Lea and Boyle, 1989; Groeneveld et al., 2018; Brinkmann et al., 2022; Guo et al., 2023). These studies often focus on species of benthic foraminifera that are 1) abundant in the studied samples, and 2) valuable as

proxy carriers since they have been used in numerous palaeoceanographic reconstructions.

Here, we analyse *in situ* Ba/Ca ratios from two species of rotaliid benthic foraminifera abundant in modern sediments of the Mediterranean Sea (including the Aegean Sea), i.e., *Uvigerina mediterranea* and *Melonis affinis*. The Aegean Sea is suitable for this study since primary productivity shows gradients with increasing values along S–N transects (Section 1.1, Fig. 1). Seven stations from several basins (water depths of 600–1500 m) within the Northern and Central Aegean seas have been selected, and core tops from surface sediments have been sampled in 0.5 to 1.0 cm vertical resolution. We investigate biologic and ecologic influences on the Ba/Ca signal from live (Rose Bengal) and dead specimens by quantifying variability of Ba/Ca across these two different species using laser ablation inductively coupled plasma mass spectrometry (LA-ICP-MS). The primary research questions related to the main hypotheses tested are: 1. Do biomineralisation processes lead to species-specific Ba/Ca?, and 2. Is Ba/Ca of infaunal benthic foraminifera species-specific due to contrasting microhabitats? We further assess the differences and similarities in signals from live and dead specimens and quantify intra-test variability of Ba/Ca, hypothesizing an influence of biomineralisation processes. Then, we compare the species-specific Ba/$Ca_{foram}$ to measured bottom water Ba/Ca from the same locality in the Northern Aegean Sea, and place these new partition coefficients in a context of existing core top and laboratory calibrations. In summary, we address biomineralisation processes and ecological aspects as underlying processes of Ba incorporation into benthic foraminiferal carbonate.
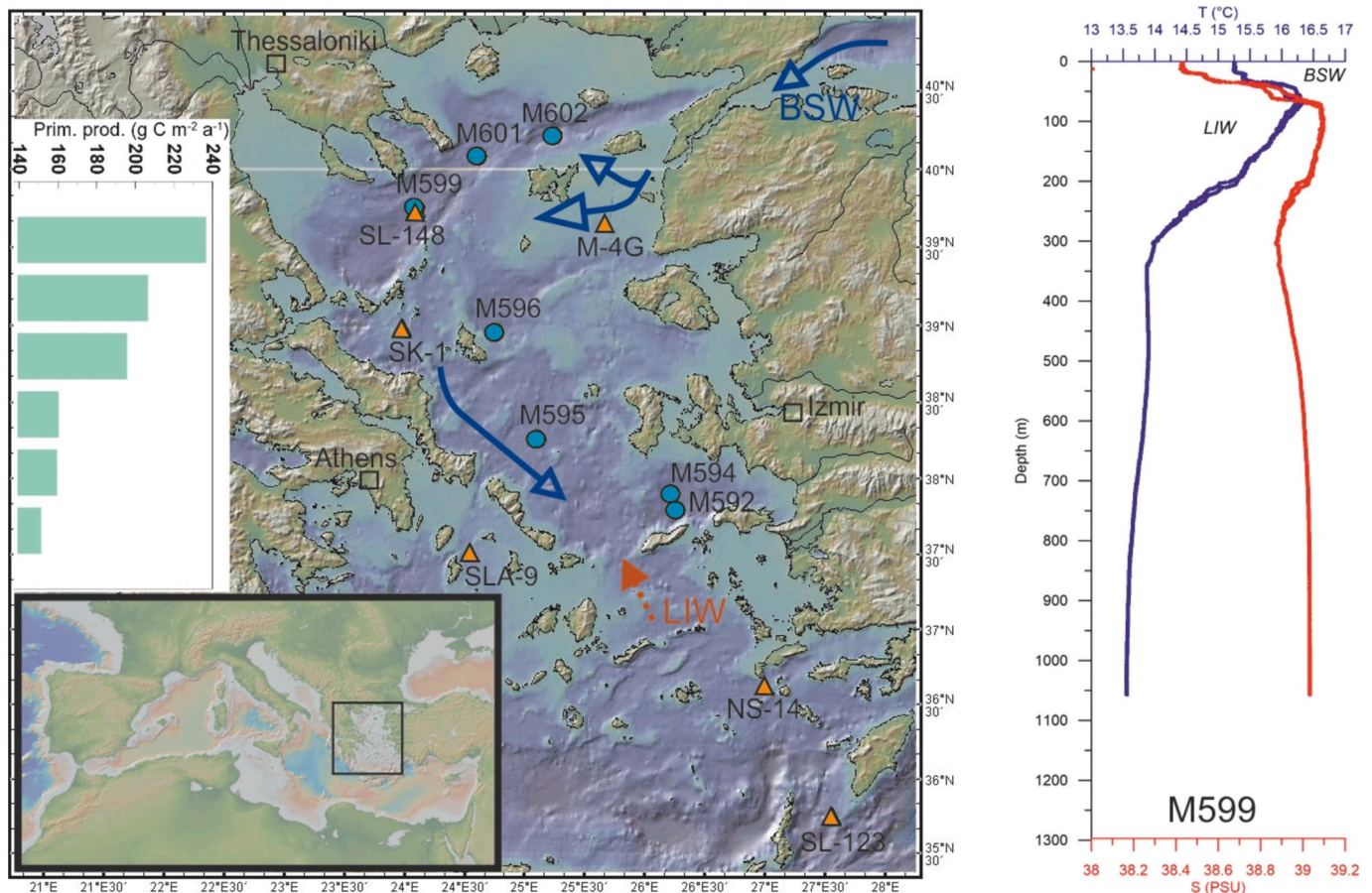


**Fig. 1.** Map of the Northern and Central Aegean seas (NAS and CAS, respectively) within the Mediterranean Sea. Sampling sites for this study are displayed by circles. M592, M594, M595, and M596 are located in the CAS whereas M599, M601, and M602 are located in the NAS. Locations of gravity cores from the Aegean Sea are displayed by triangles. Created with GeoMapApp (version 3.6.15) using topography and bathymetry of SRTM30 (Becker et al., 2009). Primary productivity data is described in Table 1, and was taken from Theodor et al. (2016a). Vertical hydrographic T and S profiles (CTD) in the Athos basin, station M599, from cruise M144 (Pross et al., 2021).

### 1.1. The Northern and Central Aegean seas as natural laboratory

The Northern and Central Aegean seas (NAS and CAS, respectively, Fig. 1) are located in the Eastern Mediterranean Sea (EMS), in connection to the Levantine Sea, and represent continental margin environments with several deep basins (Poulos, 2009). The marine environment receives freshwater inflow through several major rivers such as the Evros in the North (Poulos, 2009). Moreover, low-saline surface water enters through the Strait of the Dardanelles and the Marmara Sea from the Black Sea (Androulidakis et al., 2012). These inputs of fresh and brackish waters influence the surface water composition of the NAS (and CAS) in terms of salinity and temperature (Pazi, 2008). Productivity and terrigenous influx form a gradient from the South Aegean Sea to the CAS and NAS, where primary production seems to be mainly influenced by Black Sea Water inflow and riverine inputs (Lykousis et al., 2002; Poulos, 2009; Skliris et al., 2010). Also within the study area, the primary production is increasing from the CAS to the NAS, i.e., from S to N (Table 1; Theodor et al., 2016a). In general, bottom waters of the study area are well oxygenated ($> 4.1$ mL/L or 5.9 mg/L or 183.1 μmol/kg) for the time period prior to sampling of the surface sediment (MedAtlas, 1997; Theodor et al., 2016a). Local upwelling events seem to concern only shallow waters from above the thermocline (Androulidakis et al., 2017). The intermediate water layer is characterized by the inflow of Levantine Intermediate Water from the south, which is warmer and more saline than the surface water (Androulidakis et al., 2012; Fig. 1). The relatively cold deep water in the NAS is formed locally and with seasonal and interannual variability leading to ventilation events in the deep basins interrupting episodes of stagnation (Zervakis et al., 2003; Pazi, 2008; Androulidakis et al., 2012). Formation of deep water in the NAS has wider implications for the Mediterranean Sea, and for a defined time period its subsequent export to the EMS is described as Eastern Mediterranean Transient (e.g., Velaoras and Lascaratos, 2005; Roether et al., 2007; Tsiaras et al., 2012).

In general, the oceanography and palaeoceanography of the Aegean Sea is well constrained (Aksu et al., 1995; Triantaphyllou et al., 2016; Bozyiğit et al., 2022). In the recent past, records of Holocene sapropel formation were found to contain evidence for oxygen-depleted bottom waters (however less severely than in other Eastern Mediterranean waters), and high export productivity (Sperling et al., 2003; Abu-Zied et al., 2008; Schmiedl et al., 2010). The palaeoenvironmental changes of the Aegean Sea, including changes in atmospheric circulation, precipitation and related riverine input, and transient development of dysoxic conditions during sapropel deposition are well understood (Casford et al., 2003; Rohling et al., 2015; Tachikawa et al., 2015). In this context, the sediment record in the NAS and CAS constitutes a robust framework to test and validate the relatively unexplored palaeo-export productivity proxy Ba/Ca of benthic foraminifera. In fact, an earlier study on benthic foraminiferal test geochemistry has investigated samples from the same surface sediments in order to calibrate the $\Delta\delta^{13}C$ signal of epifaunal (*Planulina ariminensis/ Cibicides pachyderma/ Cibicides lobatulus*) and infaunal (*Uvigerina mediterranea*) benthic foraminifera for reconstructing changes in palaeo-export productivity (Theodor et al., 2016a). We are using the same set of environmental parameters (e.g., $C_{org}$ for export flux of organic carbon to bottom waters) for evaluating the variability in surface and export productivity in the study area (Table 1).

## 2. Material & methods

### 2.1. Sampling of benthic foraminifera

During R/V METEOR cruise M51/3 in November/December 2001 (Hemleben et al., 2001), a multicorer was deployed to retrieve cores from sediment surfaces at multiple locations in the different basins of the Aegean Sea. For this study we selected cores from seven stations in the Northern and Central Aegean seas (Fig. 1). Onboard the ship, the multicores were sampled for benthic foraminifera using slices of sediment. The upper 3 cm of sediment were sliced into the following intervals: 0–0.5, 0.5–1, 1–2, 2–3 cm. To each sample a solution of Rose Bengal and ethanol (1.5 g of Rose Bengal per 1 L of ethanol, 96 %) was added in order to stain specimens of benthic foraminifera alive at the time of sampling (Walton, 1952; Lutze and Altenbach, 1991; Bernhard, 2000). For our study, we chose samples which have been treated by Theodor et al. (2016a) in the following way: Samples were washed and wet sieved over a sieve with a mesh size of 63 μm before being left to dry (40 °C). The residues were sieved with a mesh size of 150 μm in order to separate coarse and fine fractions. For our study we use benthic foraminifera from the coarse fraction ($> 150$ μm). Specimens of *Uvigerina mediterranea* and *Melonis affinis* (supp. mat.; Table S1) were picked under a stereo microscope. In order to identify living specimens of both species, the following criterion was applied: only specimens with cytoplasm stained brightly by Rose Bengal in at least three subsequent chambers were considered alive (supp. mat.; Fig. S16). Consequently, the remaining specimens not fulfilling this criterion were considered dead. In total, 136 specimens were selected for subsequent analyses of elemental composition. Of those 136 specimens, there are 30 live, and 38 dead specimens of *U. mediterranea*, as well as 29 live, and 39 dead specimens of *M. affinis* (see Table 2 for the number of specimens per site in the final data set).

### 2.2. Cleaning of benthic foraminiferal tests

The protocol for the cleaning procedure of individual benthic foraminiferal tests is based on published protocols for preparation of elemental analyses by Barker et al. (2003), Glock et al. (2012, 2016), Mojtahid et al. (2019), van Dijk et al. (2019), Petersen (2017), and Petersen et al. (2018, 2019). Furthermore, this protocol agrees with cleaning procedures employed for LA-ICP-MS analyses or other microanalytical techniques employing precise targeting of parts of foraminiferal shells (with the exception of the first named study which used a wet chemical measurement method) of planktic foraminifera (from

**Table 1**

Name and location (decimal degrees, WGS84) as well as water depth of sampling stations. Environmental parameters from Theodor et al. (2016a): $C_{org}$ flux and primary production (PP), Total organic carbon (TOC); $CaCO_3$ was removed from samples, analytical precision of 0.02 %, data from Theodor et al. (2016a) and Möbius et al. (2010), and redox boundary depth. $C_{org}$ export fluxes after Betzer et al. (1984) and Antoine and Morel (1996). PP values (annual averages for the year prior to sampling); data from GlobColour project. The mean living depth (MLD) was calculated by Theodor et al. (2016a) for living specimens of *Uvigerina mediterranea* following the procedure presented by Theodor et al. (2016b).

| Station | Lat. (° N) | Long. (° E) | Depth (m) | $C_{org}$ (g C m$^{-2}$a$^{-1}$) | PP (g C m$^{-2}$a$^{-1}$) | TOC (%) | Redox depth (cm) | MLD$_{U.\ med.}$ (cm) |
|---|---|---|---|---|---|---|---|---|
| M(MUC)592 | 37.794 | 26.262 | 1148 | 5.81 | 151.46 | 0.63 | 16 | 0.38 |
| M(MUC)594 | 37.902 | 26.218 | 991 | | | | | |
| M(MUC)595 | 38.261 | 25.103 | 662 | 8.84 | 159.63 | | 19 | 0.56 |
| M(MUC)596 | 38.955 | 24.753 | 884 | 7.43 | 160.5 | 0.73 | 30 | 0.41 |
| M(MUC)599 | 39.756 | 24.094 | 1084 | 8.66 | 195.88 | 0.58 | 16.5 | 0.47 |
| M(MUC)601 | 40.087 | 24.610 | 977 | 9.97 | 206.68 | 0.75 | 6 | 0.27 |
| M(MUC)602 | 40.217 | 25.240 | 1466 | 9.36 | 236.78 | 0.82 | 4 | 0.78 |

**Table 2**

Ba/Ca ratios in µmol/mol for all analysed chambers and specimens after Laser Ablation-ICP-MS data processing (section 2.3.1). Separated for species, station, and between live and dead specimens. Reported are median and MAD (see section 2.5) with the respective number of data points, i.e., single chamber measurements (n) for all analysed specimens per station. Also reported are the number of analysed specimens (N) for each station (after LA-ICP-MS data processing). The total number of analyses represented in this table is 396.

| | Ba/Ca *U. med.* live | | n | N | Ba/Ca *U. med.* dead | | n | N | Ba/Ca *M. aff.* live | | n | N | Ba/Ca *M. aff.* dead | | n | N |
|---|---|---|---|---|---|---|---|---|---|---|---|---|---|---|---|---|
| | median | MAD | | | median | MAD | | | median | MAD | | | median | MAD | | |
| MUC592 | 1.57 | 0.25 | 13 | 3 | 1.82 | 2.42 | 63 | 13 | 2.44 | 0.36 | 6 | 2 | 2.76 | 0.39 | 19 | 8 |
| MUC594 | 2.03 | 0.41 | 9 | 3 | 1.56 | 0.14 | 12 | 4 | 3.68 | 4.84 | 5 | 2 | 5.41 | 2.17 | 9 | 5 |
| MUC595 | 1.98 | 1.06 | 20 | 4 | | | | | 2.88 | 0.16 | 4 | 3 | | | | |
| MUC596 | 1.93 | 0.98 | 21 | 7 | 1.94 | 0.46 | 18 | 6 | 16.90 | 9.54 | 6 | 2 | 4.65 | 1.12 | 11 | 6 |
| MUC599 | 1.70 | 0.22 | 30 | 6 | 1.87 | 0.44 | 25 | 5 | 2.58 | 0.58 | 5 | 2 | 2.60 | 0.71 | 17 | 6 |
| MUC601 | 2.57 | 0.12 | 9 | 3 | 2.33 | 0.45 | 21 | 7 | 8.62 | 2.02 | 8 | 4 | 3.31 | 1.38 | 12 | 7 |
| MUC602 | 2.11 | 0.25 | 20 | 4 | 1.87 | 0.15 | 15 | 3 | 4.05 | 1.13 | 12 | 4 | 3.36 | 0.25 | 6 | 3 |
| all stations | 1.93 | 0.52 | 122 | 30 | 1.88 | 0.50 | 154 | 38 | 3.90 | 2.60 | 46 | 19 | 3.18 | 0.96 | 74 | 35 |

culturing experiments and sediment trap samples; Lea and Spero, 1992; Vetter et al., 2013; Spero et al., 2015; Branson et al., 2016; Richey et al., 2022). Regarding Na/Ca, similar sample preparation and cleaning methods have been used by Mezger et al. (2018) when analysing planktic foraminifera from core tops. First, specimens were put in vials and rinsed three times with reverse osmosis water (ROW). During each rinsing step, the vials were put into an ultrasonic bath for approx. 20 s. Afterwards, the vials were rinsed three times with methanol and put into the ultrasonic bath for 1 min during each rinsing step. The vials were rinsed again two times with ROW to remove residual methanol (in an ultrasonic bath for approx. 2*20 s). In order to remove organic matter adhering to the tests, an oxidative reagent was freshly mixed by adding 100 µL 30 % $H_2O_2$ to 10 mL of a 0.1 M NaOH solution. Subsequently, 350 µL of this reagent were added to each vial. The vials were transferred into an approx. 75 °C warm water-bath (with ultra-sonication) for 15 min to remove contamination by organic matter. During this oxidative cleaning step, samples were removed from the water-bath in 5 min intervals to remove gas bubbles by tapping the bottom of the vials. After 15 min the foraminiferal specimens were rinsed with ROW. The oxidative cleaning was repeated once. Finally, the vials were rinsed twice with ROW to remove residues of the reagent. All specimens were picked from vials and left to dry on slide.

### 2.3. Analyses by Laser Ablation ICP-MS

We measured the elemental composition of single chambers of the calcite tests using LA-ICP-MS at the Institute of Geosciences, at the University of Mainz, Germany. The analytical setup involves an ArF excimer laser (193 nm, ESI New wave) which is coupled to a quadrupole ICP-MS (Agilent 7500ce). Ablations were performed in a TwoVol$^2$ 2-Volume Cell with He as carrier gas, a laser energy density of 2–3 J/cm$^2$ and a 7 Hz repetition rate. Foraminiferal samples were ablated with an energy density of 2 J/cm$^2$ and, reference materials at a slightly higher energy density of ~3 J/cm$^2$. Spot sizes of spot ablations, sampling vertically through the sample material, were 50 µm in diameter for foraminifera and reference materials. The ICP-MS settings included an RF Power of 1200 W, a sampling depth of the torch of 6 mm, and a gas-flow rate (Ar) of 0.86 (L/min). Before the start of each measurement session ($n = 2$ different sessions), the ICP-MS was tuned to monitor elemental fraction effects by ensuring a U/Th of ~1. The oxide formation was monitored as well by ensuring a low ThO$^+$/Th$^+$ ratio (< 0.5–0.8 %). A background signal of 15 s was recorded before the measurement of each laser ablation profile which lasted for 30 s. The analysed isotopes were: $^{23}$Na, $^{25}$Mg, $^{26}$Mg, $^{27}$Al, $^{43}$Ca, $^{55}$Mn, $^{56}$Fe, $^{66}$Zn, $^{88}$Sr, $^{137}$Ba, $^{138}$Ba, $^{140}$Ce, and $^{208}$Pb. The dwell time for each analyte (isotope) was set to 10 ms.

The data were calibrated against NIST SRM 610. The calibration using NIST SRM 610, or NIST glasses in general, was shown to yield accurate results for carbonates (e.g., Jochum et al., 2012, 2019).

Fractionation effects were monitored using different reference materials (USGS MACS-3, NIST SRM 612, and BCR-2G), which were analysed after each block of 30 ablations of sample material. For the calculation of element concentrations, the GLITTER software was used with $^{43}$Ca as internal standard, assuming samples contained 40 wt% Ca of CaCO$_3$ (e. g., Petersen et al., 2018). External reproducibility for Ba/Ca was determined using carbonate reference materials USGS MACS-3 as 1.1 % (calculated as 2xRSE, relative standard error, based on the average value of 59.4 ppm and a standard deviation of 2.4 ppm for $n = 51$ measurements of all analytical sessions). A table for external reproducibility of Ba, Mg, Sr, and Na is given in the supplementary material (supp. mat.; Table S2).

Accuracy of Ba/Ca was also ensured via comparison to the reference value of LA-ICP-MS measurements of USGS MACS-3 (mean ± SD: 58.9 ± 1.9 ppm) established by Jochum et al. (2012). Analyses were performed in the penultimate (n-1), antepenultimate (n-2), and n-3 chambers of individuals of *U. mediterranea* and *M. affinis*, as well as up to n-7 chambers in a subset of individuals of *U. mediterranea*.

### 2.3.1. Laser Ablation ICP-MS data processing

Laser ablation data processing includes several steps of data reduction. Since the data were acquired by ablating vertically through the shell in a time-resolved way (Figs. S10 and S11), a stable count of Ca implies that these parts of the ablation profiles included the analysis of the entire test wall, and such zones were selected for further interpretation (e.g., Petersen et al., 2018; Brinkmann et al., 2022). Having performed these steps for all analysed profiles, we have excluded parts of profiles with elevated raw data values for elements that can or could be associated with coatings on the outside and inside of shell walls (Al, Fe, Zn, and to a lesser extent Mn). This step was performed within the software Glitter based on visual inspection of the profiles. Implicitly, this data reduction proofs that final data sets show Ba/Ca ratios of the foraminiferal carbonate which are not influenced by other phases of Ba, also validating our cleaning method described in section 2.2 (e.g., Spero et al., 2015; Mojtahid et al., 2019; Ni et al., 2020; Brinkmann et al., 2022; Guo et al., 2023). Moreover, in the resulting data set of calibrated concentration values (ppm) we have removed all profiles with 1) remaining (after data reduction and selection of integration interval within the Glitter software) exceptionally high concentrations of Al (> 200 ppm, or ~ 700 µmol/mol), Fe (> 300 ppm, or ~ 500 µmol/mol), and Mn (> 200 ppm, or ~ 350 µmol/mol), and 2) profiles for which the integration interval within the ablation profile included not sufficient data points for reliable calibration/quantification (< 10 sweeps, i.e., data points, of the ICP-MS). These steps of scrutinizing laser ablation profiles were adapted on the basis of previous protocols of LA-ICP-MS data of benthic and planktic foraminifera from culturing experiments, core tops and down core records published in Petersen (2017), Petersen et al. (2018), Petersen et al. (2019), Barras et al. (2018), Mojtahid et al. (2019), Nairn et al. (2021), Guo et al. (2019), Brinkmann et al. (2022),

de Nooijer et al. (2017), Ní Fhlaithearta et al. (2010), Wit et al. (2010), Marr et al. (2011), Leduc et al. (2014), and Reichart et al. (2003). Moreover, for setting the thresholds in Al, Fe, and Mn, we employed histograms and boxplots shown in Figs. S12 to S15 of the supplementary material. In this way, the data set was reduced from originally 456 to 396 data points. We ensured that all data were above limits of quantification for Na, Mg, Ba, and Sr.

### 2.4. Sea water analyses

Sea water samples from R/V METEOR cruise M144 (December 2017) sampled at station M599 of R/V METEOR cruise M51 (December 2001) were analysed for concentrations of Ca, Mg, Na, and Sr by a Thermoscientific iCap ICP-OES Duo 6300 at the Institute of Geosciences, University of Frankfurt. Samples were diluted 40:1 with $HNO_3$. Yttrium was used as an internal standard element with a concentration of 1 mg/L. Intensity data was background corrected and standardized to Y. IAPSO and NASS-7 seawater reference materials were measured to allow for drift correction and monitor measurement quality. Accuracy is reported as the deviation of the measured reference materials from reported values and amounts to 97 %, 101 %, 99 % and 108 % for Ca, Mg, Na and Sr. Precision is reported as the RSD of the measured reference materials ($n = 3$) and amounts to 1.5 %, 1.1 %, 2.4 % and 1 % for Ca, Mg, Na and Sr.

Seawater samples were analysed for Ba by a Thermoscientific Sector Field Element ICP-MS. Samples were diluted 1:1 with $HNO_3$. Yttrium was used as an internal standard element with a concentration of 0.025 mg/L. Intensity data was background corrected and standardized to Y. IAPSO, NASS-7 and Multi-Element Standard Solution were measured after every 8th sample to allow for drift correction and monitor measurement quality. Accuracy is reported as the deviation of the measured reference materials from reported values and amounts to 93 % for Ba. Precision is reported as the RSD of the measured reference materials ($n = 4$) and amounts to 2.8 % for Ba.

### 2.5. Statistical analyses

Statistical analyses were performed in R (R Core Team, 2016) version 3.5.2 with RStudio (version 1.1.463) and graphical representations were generated using ggplot2 (Wickham, 2009). Statistical tests included testing against normal distribution using Kolmogorov-Smirnov tests. For non-normally distributed data, subsets were tested for significant differences using Kruskal-Wallis tests (including post-hoc tests). Non normally distributed data is reported with median values and median average distances (MAD) in order to compare subsets. When comparing Ba/Ca ratios to the measured environmental parameters, in order to check for potential correlations of both parameters, we used Spearman rank correlation. In all cases, a $p$ value below 0.05 was considered as significant.

### 3. Results

#### 3.1. Ba/Ca of live and dead specimens

For *Uvigerina mediterranea*, there are no significant differences between live and dead specimens (median ± MAD: 1.93 ± 0.52 for $n = 122$, and 1.88 ± 0.50 μmol/mol for $n = 154$, respectively; Table 2, and Figs. 2, 3). For *Melonis affinis*, there are significant differences between live and dead specimens (median ± MAD: 3.90 ± 2.6 for $n = 46$, and 3.18 ± 0.96 μmol/mol, for $n = 74$, respectively; Table 2, and Figs. 2, 4). Altogether, the Ba/Ca of live *M. affinis* is elevated compared to dead specimens (significant difference, Kruskal Wallis rank sum test $p$ value = 0.0081). This effect is due to results from two stations (M596 and M601) of which one (M596) shows values >9.1 μmol/mol (median + 2*MAD for all data of live specimens of *M. affinis*, i.e., threshold for identifying high values) for live specimens. When these high values are omitted ($n = 10$), there is no significant difference between live and dead specimens of *M. affinis* ($p$ value = 0.1371).

#### 3.2. Foraminiferal Ba/Ca between sampling sites

For live specimens of *U. mediterranea*, average (median of all single chamber Ba/Ca) values per station range from 1.57 ± 0.25 for $n = 13$ (M592) to 2.57 ± 0.12 for $n = 9$ (M601) μmol/mol (Table 2, and Figs. 3 and 5). For dead specimens of *U. mediterranea*, average values per station show a variability from 1.56 ± 0.14 for n = 12 (M594) to 2.33 ± 0.45 for $n = 21$ (M601) μmol/mol (Table 2, and Figs. 3 and 5). For the live specimens of *M. affinis*, the range of average values is from 2.44 ± 0.36
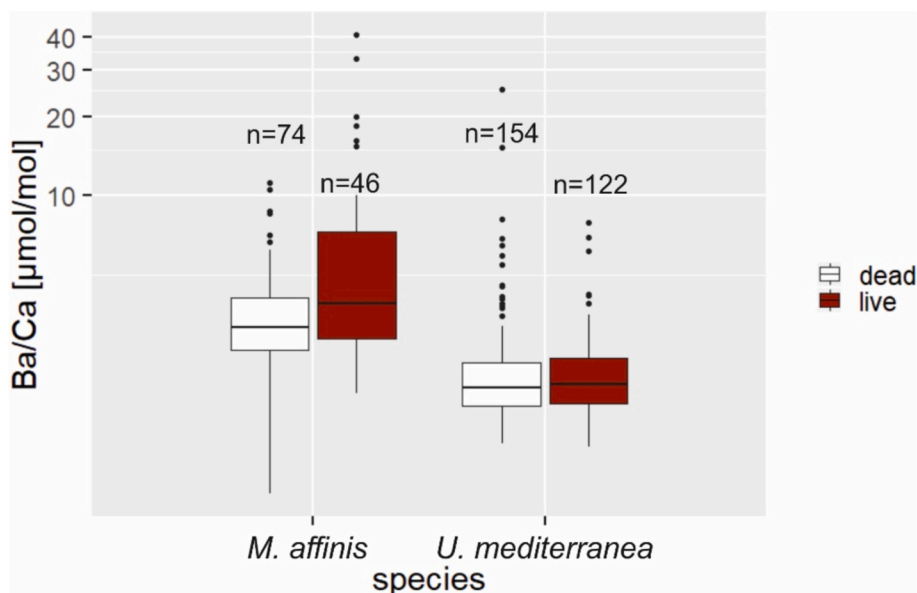


**Fig. 2.** Ba/Ca ratios of all analysed chambers and specimens (see Table 2). Results are reported as boxplots per species, and separated between live and dead specimens. Number of analyses per boxplot are given, i.e., single chamber values.
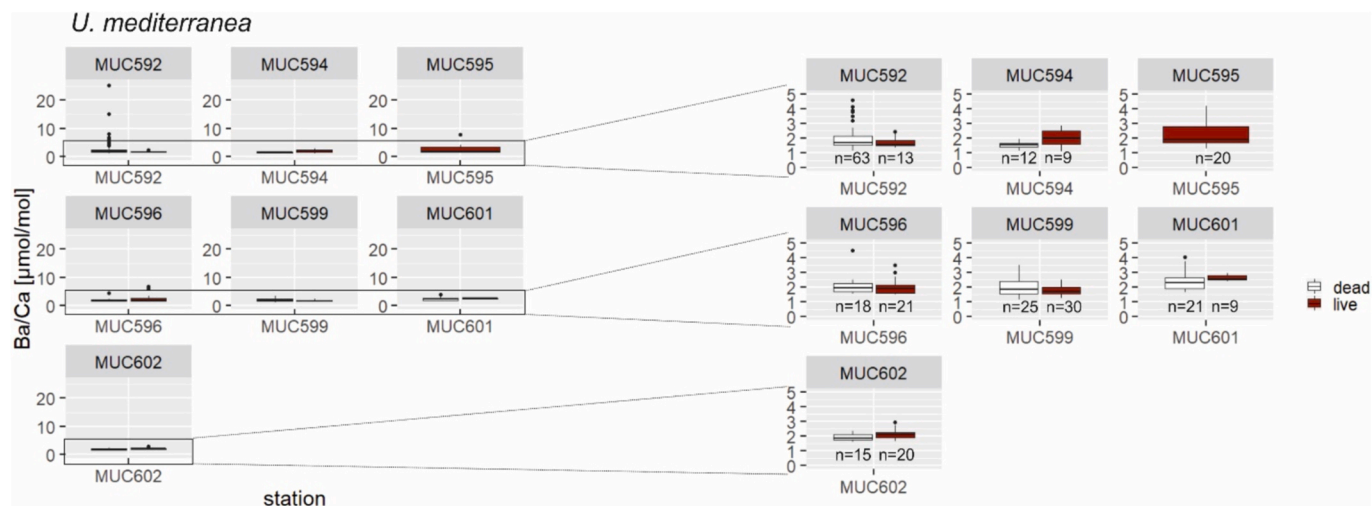
**Fig. 3.** Ba/Ca ratios of *U. mediterranea*. Results are reported as boxplots per station, and separated between live and dead specimens (see Table 2). For panels on the right half the data was cropped to values ≤5 μmol/mol. Number of analyses per boxplot are given, i.e., single chamber values.
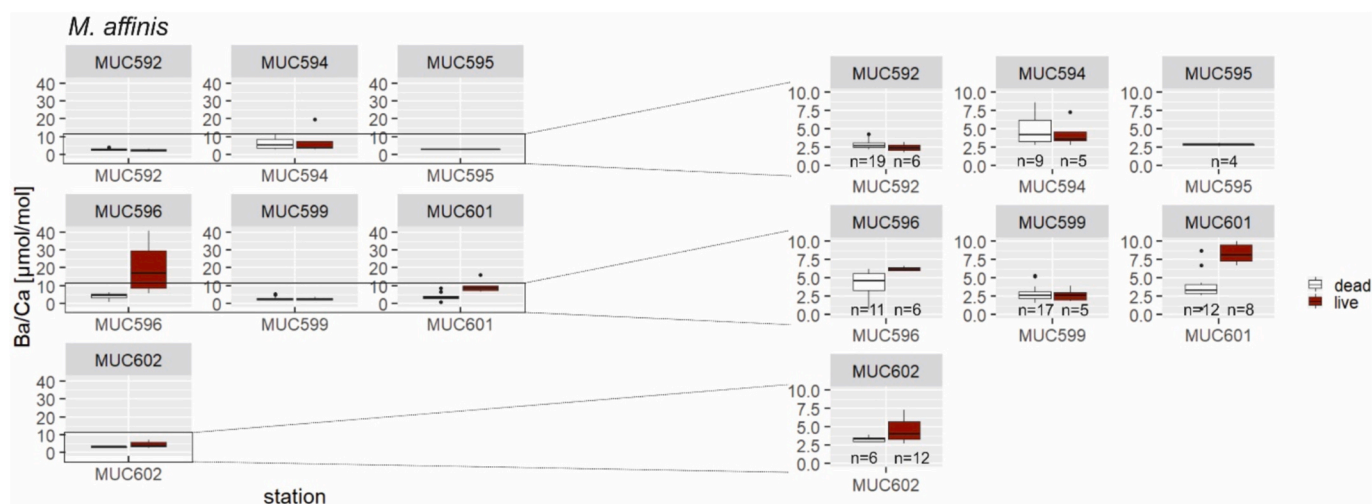


**Fig. 4.** Ba/Ca ratios of *M. affinis*. Results are reported as boxplots per station, and separated between live and dead specimens (see Table 2). For panels on the right half the data was cropped to values ≤10 μmol/mol. Number of analyses per boxplot are given, i.e., single chamber values.

for $n = 6$ (M592) to 16.90 ± 9.54 for n = 6 (M596) μmol/mol (Table 2, and Figs. 4 and 5). For the dead specimens of *M. affinis*, the average values range from 2.60 ± 0.71 for $n = 17$ (M599) to 5.41 ± 2.17 for n = 9 (M594) μmol/mol (Table 2, and Figs. 4 and 5). The range of Ba/Ca within single stations is relatively high, and the inter-station comparison is not resulting in a marked south to north gradient of Ba/Ca for *U. mediterranea* (Fig. 5). Thus, there are no meaningful correlations to the environmental parameters shown in Table 1 for which a S to N increasing gradient may be apparent (e.g., Ba/Ca vs. $C_{org}$ flux; Spearman rank correlation; *rho* = 0.27 with *p* value <0.001, for $n = 276$ data points of combined live and dead Ba/Ca; note that individual inter-station comparisons of Ba/Ca ratios yield significant differences, without a repeated pattern between live and dead specimens). Similarly, the dead specimens of *M. affinis* show no particular trend with latitude in inter-station comparison of Ba/Ca and thus no significant correlation to any observed environmental variable (e.g., $C_{org}$ flux; *rho* = 0.19 with *p* value<0.04, for $n = 120$ data points of combined live and dead Ba/Ca). However, the median Ba/Ca of live specimens of *U. mediterranea* is highest (and Ba/Ca of live specimens of *M. affinis* is affected by high values at station M596 and) at station M601 which shows a relatively low value in redox boundary depth (6 cm) and a high value in $C_{org}$ flux (9.97 g C m$^{-2}$a$^{-1}$; Table 1).

### 3.3. Species-specific Ba/Ca

*U. mediterranea* has a lower range of Ba/Ca than *M. affinis*. For *U. mediterranea*, the majority of values is in the range ≤ 5 μmol/mol, while for *M. affinis* values stretch further up with numerous counts in the range ≤ 10 μmol/mol, as shown in the histograms for live and dead specimens separately (Fig. 6). When using non-parametric tests (Kruskal Wallis rank sum test), the difference between both species in Ba/Ca for live specimens is significant (*p* value <6 × 10$^{-16}$, for $n = 168$ data points of live specimens from both species) as well as for dead specimens (*p* value <2.2 × 10$^{-16}$, for $n = 228$ data points of dead specimens from both species). Even if high Ba/Ca values are excluded from the live data (as the data for *M. affinis* suggests that outliers could influence the result, we removed all values exceeding the median + 2*MAD for this subset: all data <9.1 μmol/mol remained in the new dataset, $n = 10$ data points are removed), the difference between both species remains significant (*p* value 8 × 10$^{-13}$).

For each station, separated between live and dead specimens, the Ba/Ca of *M. affinis* displays elevated average values compared to *U. mediterranea* (Fig. 5). At individual stations, the Ba/Ca has been plotted per sampling depth (Figs. 7, 8, for stations M599 and M602, respectively; for all other stations plots are found in the supplementary
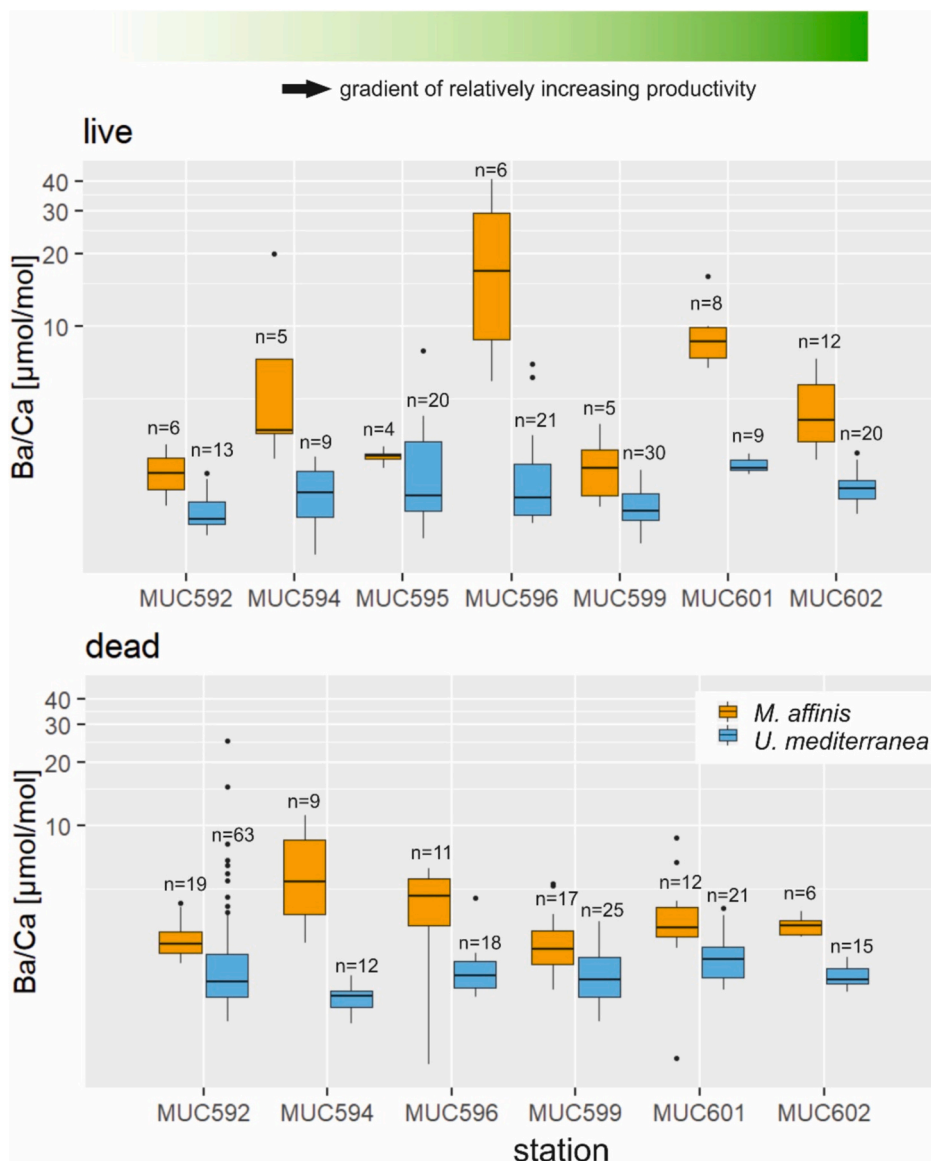
**Fig. 5.** Ba/Ca ratios of live specimens (above) and dead specimens (below) reported as boxplots per station, and per species (n for number of analyses per boxplot, i. e., single chamber values, cf., Table 2). Indicated above is the gradient of relatively increasing productivity (PP and C$_{org}$ flux, cf., Table 1).
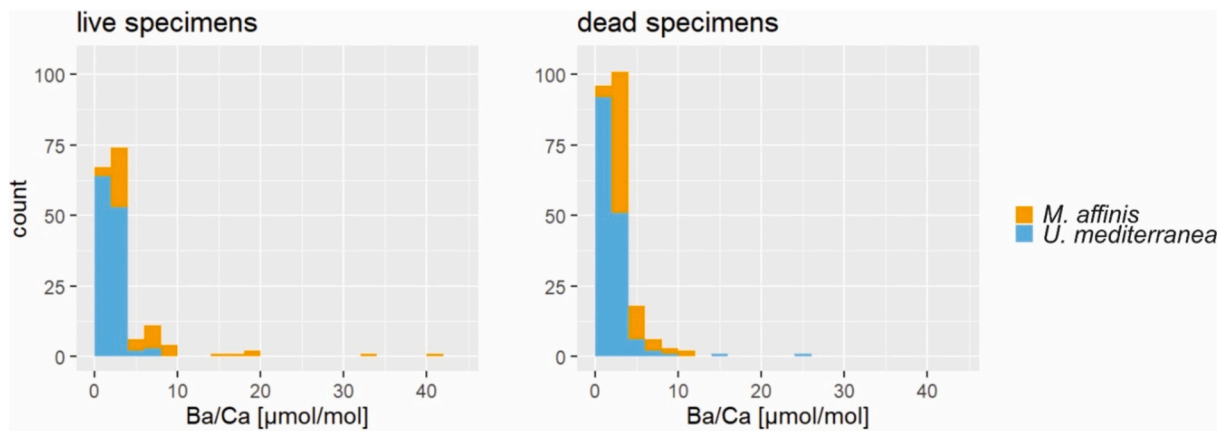


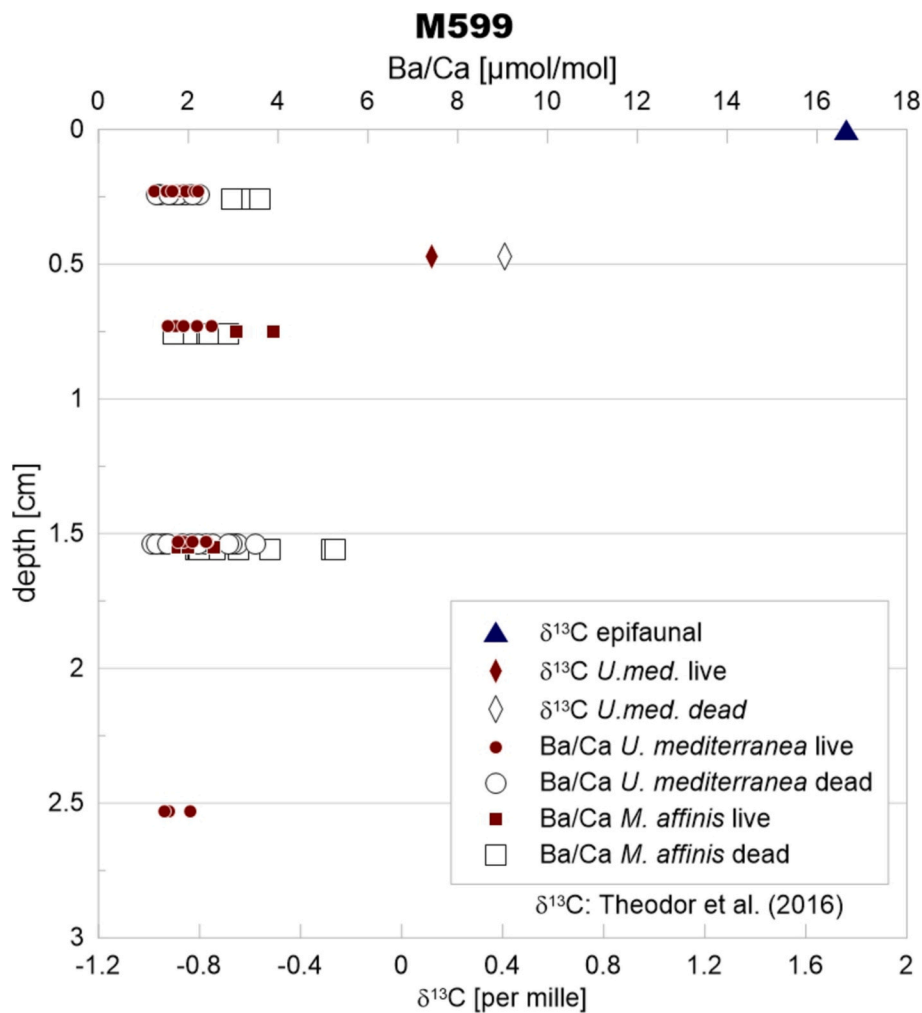**Fig. 6.** Histogram for all single chamber Ba/Ca ratios of live specimens (left) and dead specimens (right).

**Fig. 7.** All single chamber Ba/Ca ratios of specimens from station M599 (this study). Different colours and symbols apply to different species. The $\delta^{13}$C ratios of *U. mediterranea*, and $\delta^{13}$C ratios of epifaunal species are shown as well (data from Theodor et al., 2016a).

material; Figs. S1–S5), also per sampling depth the values for Ba/Ca of *M. affinis* have a range of elevated values compared to those of *U. mediterranea* (both for live and dead specimens) at most stations.

### 3.4. Ba/Ca intra-test variability

The Ba/Ca intra-test variability expressed as relative standard deviation in % (RSD=SD*100/average) for each specimen is shown in Table 3. For *U. mediterranea*, 3 to 5 chambers per individual have been analysed. For *M. affinis*, 2 to 3 chambers per specimen have been analysed (specimens with only 1 chamber passing criteria of data processing have been omitted for this comparison). For live and dead specimens of *U. mediterranea*, intra-test variability is 16 ± 12 and 19 ± 19 % on average, respectively (Table 3). For live and dead specimens of *M. affinis*, intra-test variability is 24 ± 17 and 16 ± 17 % on average, respectively. In order to compare the Ba/Ca intra-test variability to intra-test variability of other elements, we show in Table 3 the results of Mg/Ca and Sr/Ca for our data. Ba/Ca and Sr/Ca chamber-to-chamber variability for live and dead specimens of *U. mediterranea* from station M599 are shown in Fig. 9 (similar plots for Ba/Ca of *U. mediterranea* from all stations in the supplementary material; Fig. S6), and show no consistent trend for Ba/Ca with ontogeny.

### 3.5. Sea water Ba concentration at sampling site M599

Samples of sea water at station M599 exhibit Ba concentrations of

50.3 ± 1.4 nmol/L for a depth of 10 m, 53.2 ± 1.5 nmol/L at 110 m depth, and 69.9 ± 2.0 nmol/L in the bottom water at 1064 m depth (corresponding to a bottom water Ba/Ca of 5.3 µmol/mol with measured [Ca], Table 4).

## 4. Discussion

### 4.1. Ba/Ca intra-test variability

In order to quantify Ba/Ca intra-test variability and provide new insights on the influence of biomineralisation processes on this factor, we have compiled the LA-ICP-MS data of individual chambers of *U. mediterranea* and *M. affinis* per specimen. We showed in Section 3.4 and Table 3 that the Ba/Ca intra-test variability is similar between live and dead specimens of *U. mediterranea* as well as for live and dead specimens of *M. affinis*. Therefore, it seems that the Ba/Ca signal from dead specimens is reflecting the same variability as live specimens, and is representative for the total fauna. While Mg/Ca intra-test variability is similarly high and variable when compared to Ba/Ca intra-test variability in both species, the Sr/Ca intra-test variability is lower by an order of magnitude (Table 3). For cultured and core top specimens of different species of benthic foraminifera, intra-test variability of Mg/Ca of 20–50 % RSD has been reported (Curry and Marchitto, 2008; de Nooijer et al., 2014a; Petersen et al., 2018). Petersen et al. (2018) concluded that 20 % Mg/Ca intra-test variability could be attributed to intrinsic factors (i.e., the combined variability resulting from vital
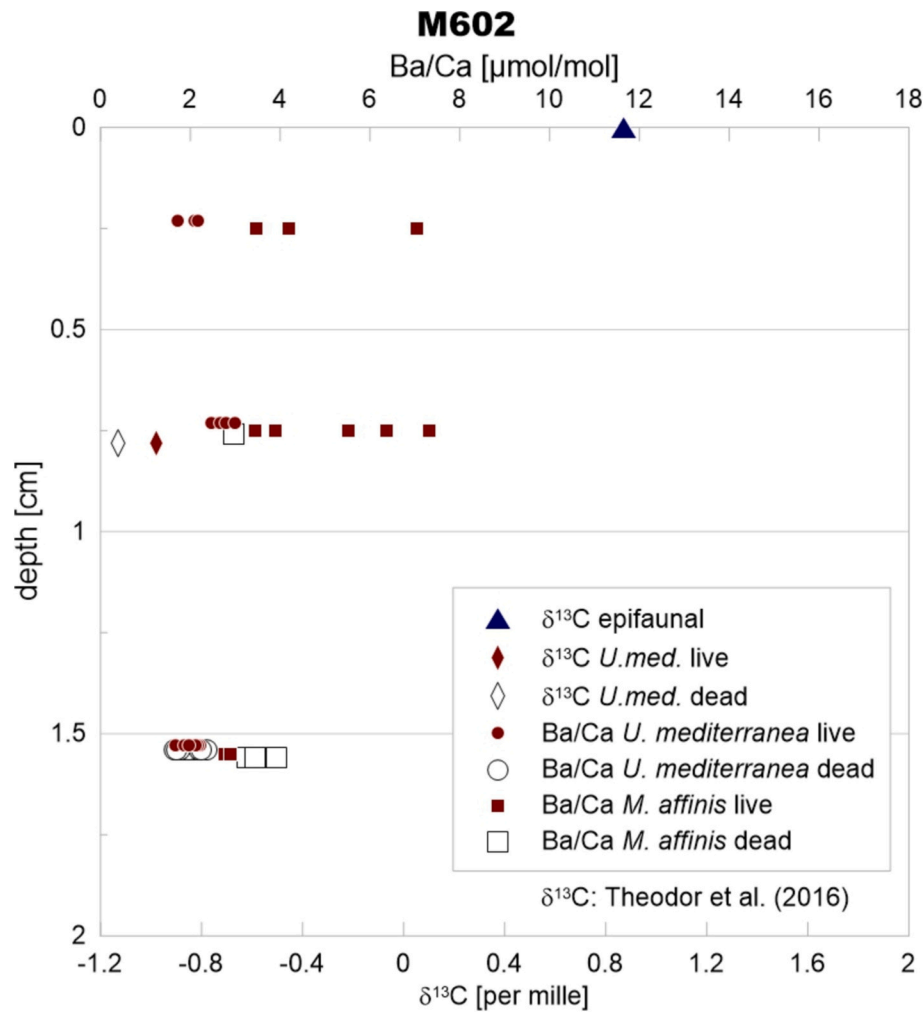
**Fig. 8.** All single chamber Ba/Ca ratios of specimens from station M602 (this study). Different colours and symbols apply to different species. The $\delta^{13}C$ ratios of *U. mediterranea*, and $\delta^{13}C$ ratios of epifaunal species are shown as well (data from Theodor et al., 2016a).

**Table 3**

Ba/Ca, Sr/Ca, and Mg/Ca intra-test variability expressed as RSD %, with average for all analysed specimens and respective SD. Number of specimens (N), as well as number of chambers per specimen (n) applies to Ba/Ca, Sr/Ca, and Mg/Ca.

| | live | | | | dead | | | |
|---|---|---|---|---|---|---|---|---|
| | **RSD % average** | RSD % SD | n = number of chambers per specimen | N = number of specimens | **RSD % average** | RSD % SD | n = number of chambers per specimen | N = number of specimens |
| | **16** | 12 | 3 to 5 | 30 | **19** | 19 | 3 to 5 | 38 |
| *U. med.* | **Ba/Ca** | | | | | | | |
| | **24** | 17 | 2 to 3 | 16 | **16** | 17 | 2 to 3 | 28 |
| *M. aff.* | **Sr/Ca** | | | | | | | |
| *U. med.* | **5** | 2 | | | **5** | 3 | | |
| | **2** | 1 | | | **3** | 2 | | |
| *M. aff.* | **Mg/Ca** | | | | | | | |
| *U. med.* | **22** | 11 | | | **21** | 13 | | |
| *M. aff.* | **16** | 19 | | | **16** | 17 | | |

effects related to biomineralisation processes during chamber growth and from ontogenetic trends, which are size-related vital effects, meaning chamber-to-chamber variability) when referring exclusively to the results of culturing experiments of de Nooijer et al. (2014a). Furthermore, Petersen et al. (2018) resumed, based on data of previous studies by Bentov and Erez (2005, 2006) and Nehrke et al. (2013) as well as following the suggestions made by de Nooijer et al. (2014b) that the Sr/Ca intra-test variability was reported with lower values (< 10 % RSD) than those for Mg/Ca in all of the aforementioned studies. This

observation allows postulating that biomineralisation processes may lead to higher intra-test variability for elements that are strongly discriminated against during the chamber forming process (e.g., Mg) than for rather passively transported ions from seawater to the site of calcification (e.g., Sr). Since we can show that the intra-test variability of Ba/Ca is of the same order of magnitude as for Mg/Ca, and higher than for Sr/Ca, we speculate that most of the intra-test variability of Ba/Ca (and Mg/Ca) of the studied specimens is related to intrinsic factors of the biomineralisation process. Support for this hypothesis comes from the
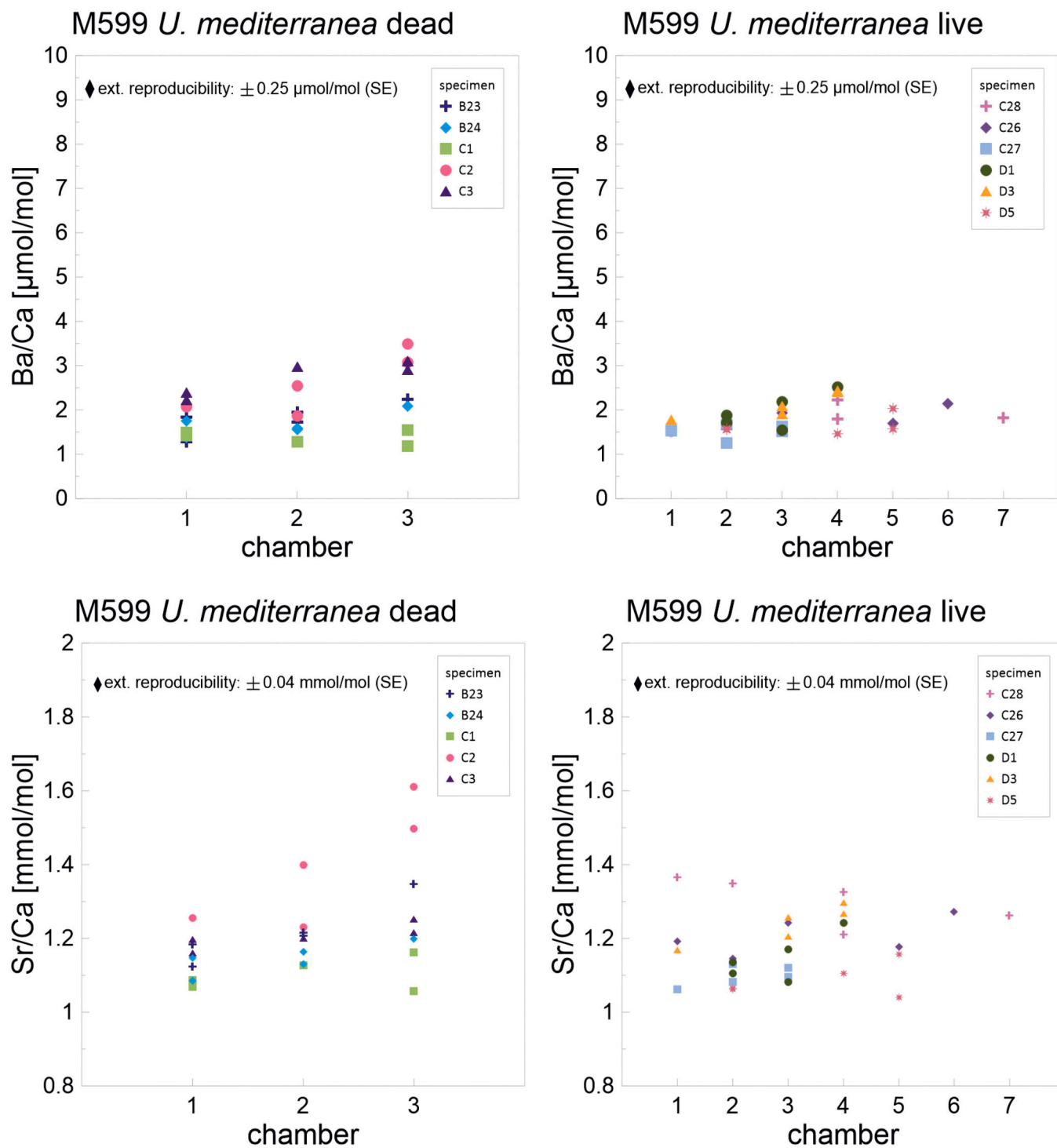
**Fig. 9.** Ba/Ca and Sr/Ca intra-test variability expressed as single chamber values per specimen for all specimens of *U. mediterranea* sampled at station M599 (live and dead specimens shown separately). Different symbols and colours apply to different specimens. The external reproducibility is applied as error bar for single chamber el/Ca.

results of Ba/Ca (and Mg/Ca, as well as Sr/Ca) ratios from a culturing experiment with large hyaline benthic foraminifera by de Nooijer et al. (2017), for which these authors associate similar biomineralisation processes as for small miliolid benthic foraminifera. A Ba/Ca intrinsic intra-test variability of 9 ± 4 %, and 13 ± 4 % can be associated with *Heterostegina depressa* and *Amphistegina lessonii*, respectively, based on Ba/Ca single chamber analyses of multiple specimens within single aquaria with constant [Ba] (de Nooijer et al., 2017). For *A. lessonii*, the Mg/Ca and Sr/Ca intra-test variability fit the pattern described above:

Mg/Ca intra-test variability is 20 ± 9 % whereas Sr/Ca intra-test variability is 6 ± 3 % (compared to a Ba/Ca intra-test variability of 13 ± 4 %). However, for *H. depressa*, Mg/Ca and Sr/Ca intra-test variability are on the same order of magnitude (6 ± 3 % and 7 ± 3 % for Mg/Ca and Sr/Ca, respectively, compared to a Ba/Ca intra-test variability of 9 ± 4 %). De Nooijer et al. (2017) argue that the Ba/Ca intra-test variability in their cultured specimens could be explained by vital effects and/or ontogenetic trends. In fact, they describe a significant decrease of Ba/Ca with chamber size (i.e., latest built chambers), and thus ontogeny, for

**Table 4**

Seawater analyses for three different water depths at station M599 sampled during cruise M144 in December 2017. Reported values are the mean of two analyses.

| Depth (m) | Ca (mmol/L) | Mg (mmol/L) | Na (mmol/L) | Sr (µmol/L) | Ba (nmol/L) | Ba/Ca (µmol/mol) |
|---|---|---|---|---|---|---|
| 10 | 13.2 | 61.5 | 518.6 | 99.6 | 50.3 | 3.8 |
| 110 | 13.3 | 62.9 | 522.6 | 101.9 | 53.2 | 4.0 |
| 1064 | 13.2 | 62.2 | 514.2 | 101.1 | 69.9 | 5.3 |

their cultured specimens of *A. lessonii* and *H. depressa*. For the data presented here, we argue that it is rather vital effects than ontogenetic trends leading to the amount of Ba/Ca intra-test variability, since for our specimens, there are no consistent ontogenetic Ba/Ca trends within single specimens (Fig. 9 for specimens from station M599, and supp. mat. Fig. S6 for specimens from all stations).

Lea and Spero (1992) analysed single shell Ba/Ca from cultured planktonic foraminifera (*Orbulina universa*) by solution ICP-MS and found that intra-test variability was within the analytical error of the method (4.4 % standard deviation) for three of five different culturing conditions. Richey et al. (2022) analysed planktic foraminifera (e.g., *Globorotalia truncatulinoides*) by LA-ICP-MS and reported Ba/Ca intra-test variability from ablation profiles of different chambers of the same specimen. The data suggests that Ba/Ca intra-test variability may range over one order of magnitude (<50–>200 µmol/mol). Therefore, it seems likely that also within planktic foraminifera, intrinsic variability assessed by LA-ICP-MS is at least as high as for benthic hyaline foraminifera. Recently, Ba/Ca measured with LA-ICP-MS was evaluated in terms of intra-test variability of live specimens from near-coastal environments, i.e. *Bulimina marginata* and *Nonionellina labradorica* (Brinkmann et al., 2022), as well as *Cribrononion subincertum* and *Florilus decorus* (Guo et al., 2024), respectively. In both studies, the authors have employed different approaches to assess Ba/Ca intra-test variability compared to the approach discussed here using a RSD per specimen. The results of Brinkmann et al. (2022) and Guo et al. (2024) show the presence of ontogenetic trends that can be overprinted by, or can be related to, temporal variability of the driving environmental factor responsible for Ba distribution in the bottom waters of the respective coastal areas.

Inorganic carbonate growth experiments (Kitano et al., 1971; Angus et al., 1979; Pingitore, 1986; Tesoriero and Pankow, 1996) indicate that the calcite lattice is less compatible with ions larger than Ca (such as Ba and Sr). These larger ions may be incorporated in an uncoordinated way in the calcite lattice (Lorens, 1981), between the actual lattice positions, leading to deformation of the calcite lattice (pointed out by Pingitore and Eastman, 1984), or be adsorbed to surfaces (Pingitore, 1986). From this point of view, we could expect to a certain extent similar behaviour and potential variability of Ba/Ca and Sr/Ca in inorganically grown calcite at similar concentrations. Since we observe a higher intra-test variability for Ba/Ca than for Sr/Ca (16–24 % RSD for Ba/Ca vs. 2–5 % RSD for Sr/Ca, on average), we may speculate that this higher intra-test variability for Ba/Ca is related to factors deriving from biomineralisation processes rather than from factors that are universal to inorganic and biogenic carbonates, and/or that the different concentrations of Ba and Sr in seawater lead to different variability in the calcite (cf., Table 4).

In conclusion, it seems that most of the Ba/Ca intra-test variability observed in our deep-sea core top specimens of benthic foraminifera is explained by intrinsic factors since it is similarly high as Mg/Ca intra-test variability, and since results from culturing experiments show similarly high values of intra-test variability. Intrinsic factors are related to biomineralisation processes (vital effects), and short-term variability (i.e., during the lifespan of a foraminifer) of environmental factors such

as export productivity seems to be of minor importance for deep-sea Ba/Ca intra-test variability.

### 4.2. Species-specific Ba/Ca

There are several possible hypotheses to explain the species-specific differences in Ba/Ca, and here we want to specifically address three of them: 1. methodological aspects, 2. biomineralisation processes, and 3. microhabitat effects. The data from this study shows significantly higher Ba/Ca for *M. affinis* than for *U. mediterranea* when all single-chamber measurements are grouped per species, and are separated between live and dead specimens (Section 3.3).

#### 4.2.1. Methodological aspects

The test walls of the two species show slight differences in ablation behaviour. In general, the ablation until perforation of the test wall lasted longer for *U. mediterranea* than for *M. affinis*. It could be argued that in the case of *M. affinis*, parts of coatings on the outside and inside of the test wall (Section 2.3.1) were included in the integration interval, leading to a bias of higher Ba/Ca for *M. affinis* compared to *U. mediterranea*. However, since laser ablation necessitates stepwise data reduction and screening for indicators of such coatings, we want to point out that these steps ensure the comparability between results of foraminiferal species that show different ablation behaviour. For our initial dataset of 456 ablation profiles of both species, the stepwise detection of anomalous data for 1) profiles with not sufficient data points (i.e., sweeps of the ICP-MS) in the integration profile and 2) extraordinary high values in the elements indicating surface contamination/ coatings, resulted in the exclusion of 60 profiles, so that 396 profiles remained. The excluded 60 profiles exclusively concern data of *M. affinis*. By removing these profiles, comparability between the remaining Ba/Ca data of both species is ensured.

Examples for such ablation profiles are given in the supplementary material (Figs. S10 and S11). For these examples, the raw data of Al (indicator of coatings) shows higher values by one order of magnitude for *M. affinis* than for *U. mediterranea*. However, the raw Ba signal for these specimens is higher in *U. mediterranea* compared to *M. affinis*. After the selection of the integration interval and calculation of elemental composition with the GLITTER software, the selected example profile for *U. mediterranea* shows a Ba/Ca of 15.2 µmol/mol compared to 0.8 µmol/mol for *M. affinis*. It should be noted that these selected examples originate from different sampling stations (M592 for *U. mediterranea*, and M601 for *M. affinis*), and in both cases, examples from the subset of dead specimens were selected.

It seems, therefore, that the slight differences in shell thickness between the two hyaline species do not necessarily lead to a bias in terms of elevated Ba/Ca ratios for *M. affinis* compared to *U. mediterranea*. However, care has to be taken when analysing and scrutinizing ablation profiles from different species in order to ensure comparability. Finally, we point out that we validated our LA-ICP-MS method against an existing Ba/Ca dataset obtained by (solution) ICP-MS (Section 4.3).

#### 4.2.2. Biomineralisation processes in benthic foraminifera

For the evaluation of our data, we consider a specific biomineralisation mixing model for benthic foraminifera that is developed by Nehrke et al. (2013), and subsequent publications (Langer et al., 2016; Barras et al., 2018; Nagai et al., 2018), and which is reassessed and put into context with other biomineralisation models (using, e.g., Rayleigh fractionation as a basis) by Nehrke and Langer (2023). This biomineralisation model mixes both processes of trans-membrane transport (TMT, selective ion channels, pumps), and passive transport (incorporation of elements from surrounding seawater at the site of calcification which was not manipulated by the foraminifer, and vacuolization of seawater; Nehrke et al., 2013). The mixing model can explain species-specific differences in el/Ca because a certain benthic foraminiferal species has a characteristic amount of passively

transported seawater (PT) that distinctively alters the el/Ca (e.g., Mg/Ca as used by Nehrke et al., 2013, and 0.04–4.4 % of PT for species used in the inter-species comparison) in comparison to a uniform el/Ca amongst different benthic foraminiferal species (and other groups of microfossils) if only TMT was driving the element incorporation.

Based on the described mixing model, we may expect for our data significant differences in the measured el/Ca between *U. mediterranea* and *M. affinis* if both species had each characteristic proportions of passively transported seawater as part of biomineralisation processes. We would expect this difference to be observable for both dead and live specimens and to act similar for all elements in the seawater (i.e., be relatively comparable in order of magnitude for all measured el/Ca). In fact, our observations show that all el/Ca (Fig. 2 for Ba/Ca; for Mg/Ca, Sr/Ca, and Na/Ca, supp. mat. Figs. S7, S8, and S9, with indicated *p* values, and the number of data points considered) are significantly different between both species for the dead specimens (i.e., in all cases the values for *M. affinis* are significantly higher than those for *U. mediterranea*). For the live specimens, there are significant differences between *U. mediterranea* and *M. affinis* for Ba/Ca and Sr/Ca, with higher values for the latter species (Fig. 2 and Fig. S8). The observed differences in Ba/Ca (and Sr/Ca) between both species for our data of live and dead specimens suggest differences in passively transported seawater to the site of calcification according to the mixing model of Nehrke et al. (2013).

However, for Mg/Ca and Na/Ca of live specimens, no significant difference between both species can be observed (Figs. S7 and S9 with indicated *p* values, and the number of data points considered). Thus, the data for Mg/Ca and Na/Ca of live specimens do not confirm the here proposed hypothesis, and speak against a systematic difference in el/Ca between both species due to biomineralisation processes. We cannot rule out that other biomineralisation processes that discriminate for certain elements may be responsible for the observed Ba/Ca (and Sr/Ca) offset between the two species. Such systematic differences may exist for the comparison of other benthic foraminiferal species and genera, and biomineralisation mixing models such as proposed by Nehrke et al. (2013) can explain many species-specific el/Ca ratios.

### 4.2.3. Microhabitat effects

This section considers species-specific microhabitat effects on Ba/Ca in the sense that pore water Ba may vary over mm to cm scales within the surface sediment. For foraminiferal species, each adapted to a preferred microhabitat (depending on organic matter fluxes and thus depth of the oxygenated zone in surface sediments and its redox boundaries; e.g., Jorissen et al., 1995; Van der Zwaan et al., 1999; Koho et al., 2008), a vertical redox zonation (and thus a gradient of pore water Ba, e.g., McManus et al., 1998; Schenau et al., 2001) would imply contrasting amounts of $Ba^{2+}$ in each microhabitat. In fact, some of the aforementioned studies have pointed out that the zone of calcification can be much narrower than the species-specific microhabitat (McCorkle et al., 1997), while others concluded that calcification could take place over longer time periods in different depths of the surface sediment (Jorissen, 2003). However, most studies imply vertical migration of benthic foraminifera in surface sediments, and calcification in (deep) macrofaunal burrows of (otherwise shallow) infaunal taxa is suggested (for occasional deep infaunal occurrences of *U. mediterranea*, Schmiedl et al., 2004). For *U. mediterranea* in comparison to *M. affinis* it has been suggested from mesocosm experiments and live census data that shallow and intermediate infaunal microhabitats can be associated, respectively (Fontanier et al., 2002; Geslin et al., 2004; Mojtahid et al., 2010). *M. affinis* is shown to be adapted to oxygen-deficient environments such as found deep in surface sediments (e.g., Licari et al., 2003; Caulle et al., 2014; Geslin et al., 2014).

From a palaeoceanographic point of view, it would be preferable to be able to relate measured el/Ca from epi- and infaunal species directly to elemental concentrations of bottom waters allowing the reconstruction of bottom water chemistry. In reality, for some elements and their

isotopic composition it has been shown that steep pore water gradients are present, and that benthic foraminiferal proxy signals may be a function of such gradients: trends in species-specific live benthic foraminiferal $\delta^{13}C$ with depth in surface sediments have been related to the preferred microhabitat depths (Fontanier et al., 2002; Tachikawa and Elderfield, 2002; Schmiedl et al., 2004), and offsets between epi- and infaunal species have been used to reconstruct export productivity (Schmiedl and Mackensen, 2006; Hoogakker et al., 2015; Lynch-Stieglitz et al., 2024). Earliest studies of fossil foraminifera have found little to no differences in foraminiferal Ba/Ca from epi- or shallow infaunal habitats (different species of cibicids compared to *Uvigerina* spp., e.g., Lea and Boyle, 1989; Lea, 1993), and it has been concluded that Ba/Ca of the epifaunal *Cibicidoides wuellerstorfi* is not influenced by pore water Ba in deep-sea surface sediments (McCorkle et al., 1995). However, a culturing study found differences in Ba incorporation between species; epifaunal *Cibicides pachyderma* incorporated more Ba for the same Ba of seawater than (shallow) infaunal *Uvigerina peregrina* as well as *Bulimina marginata* (Section 4.3; Havach et al., 2001). Mojtahid et al. (2019) have observed significant differences in Ba/Ca for different species of benthic foraminifera from samples of a sediment core covering the sapropel layer S1 (at 550 m water depth in the Eastern Mediterranean Sea). The sampled species of *Hanzawaia boueana*, *Gyroidina altiformis*, *Gyroidina orbicularis*, *U. peregrina*, and *Globobulimina affinis* can be associated to very contrasting microhabitats. Yet, a systematic trend of Ba/Ca vs. microhabitat depth was not observed, which led Mojtahid et al. (2019) to postulate that only a combination of several factors can be responsible for the observed species-specific Ba/Ca. To our knowledge, no study has so far investigated the Ba/Ca of live specimens of different species from deep-sea core tops (except for unpublished results of Martin et al. cited in McCorkle et al., 1995).

Regarding pore water profiles of Ba, published data suggests that higher Ba can be observed at greater depth and oxygen deficiency due to sulphate reduction and associated barite dissolution, as well as dissolution of Mn/Fe oxyhydroxides (e.g., McManus et al., 1998; Schenau et al., 2001). In view of these trends in pore water Ba, we would expect deeper infaunal species (e.g., *M. affinis*) to display higher Ba/Ca than shallow infaunal species (e.g., *U. mediterranea*) if the pore water Ba was substantially influencing the Ba/Ca of infaunal benthic foraminifera. This described trend is observed for Ba/Ca of our live (and dead) specimens of *U. mediterranea* compared to *M. affinis*; at stations M599 and M602 as well as at other sampled stations there is a clear tendency for Ba/Ca ratios of the latter having higher values than for the former (Table 2, Figs. 7 and 8, and supp. mat. Figs. S1–S5). Moreover, we would expect this potential microhabitat effect to exert a larger control on Ba/Ca differences between shallow and intermediate to deep infaunal species in surface sediments with narrow redox boundary depth (i.e., were oxygen is more deficient), since such environments can show a stronger pore water gradient (McManus et al., 1998), and the microhabitat of *U. mediterranea* should be restricted to a narrower zone compared to sediments with larger depths of the redox boundary (Theodor et al., 2016a). For our stations with the shallowest redox boundary depths (6 and 4 cm for M601 and M602, respectively, Table 1), we observe the most pronounced differences (for individual sampling depths, which include low numbers of data points in some cases) in Ba/Ca ratios between live specimens of *U. mediterranea* and *M. affinis* (Fig. S5 and Fig. 8, respectively).

If our here discussed hypothesis of infaunal Ba/Ca being influenced by the microhabitat depth holds true, then we would also expect a relationship/gradient between the epifaunal and infaunal Ba/Ca, similar to what has been observed for Cd/Ca of benthic foraminiferal tests (Tachikawa and Elderfield, 2002). However, as pointed out before in this section, there is evidence from the Eastern Mediterranean Sea that epifaunal Ba/Ca may not always be lower than infaunal Ba/Ca, since Mojtahid et al. (2019) observe significantly higher Ba/Ca for two species of *Gyroidina* compared to *U. peregrina* (similar as what has been observed for epifaunal and infaunal species in culturing experiments of Havach

et al., 2001). It can be argued that *Gyroidina* is not always occupying a truly epifaunal habitat and may also occupy a shallow infaunal habitat, being found in low oxygen environments of the NAS (Ní Fhlaithearta et al., 2010). In addition, for the geochemical composition of *U. peregrina* strong vital effects (or microhabitat effects) have to be considered (e.g., Schmiedl et al., 2004; Theodor et al., 2016b; Le Houedec et al., 2020).

In view of these (contrasting) findings, we think there is evidence for and against interpreting our observed differences in Ba/Ca between *U. mediterranea* and *M. affinis* as a microhabitat effect in the sense that the deeper living species reflects higher pore water Ba. Future research could address this question by investigating Ba/Ca of live specimens from core tops for a range of species known to inhabit contrasting microhabitats alongside *in situ* measurements of pore waters (Section 4.4.).

### 4.2.4. Species-specific Ba/Ca; evaluation of discussed aspects

Based on our data, hypothesis 1 (Section 4.2.1) regarding analytical aspects can be mostly rejected, whereas hypothesis 2 (Section 4.2.2) considering biomineralisation processes, and hypothesis 3 (Section 4.2.3) addressing species-specific microhabitat effects seem more promising in order to explain the species-specific effects on Ba/Ca. However, incorporation of other elements (Mg/Ca, and Na/Ca) may contradict hypothesis 2, and published data from multi-species benthic foraminiferal Ba/Ca does not confirm the here proposed microhabitat effect in relation to pore water Ba trends within the sediment surface (hypothesis 3). It remains difficult to disentangle the different possible factors, also due to the fact that there could be linkages between them.

### 4.3. Species-specific comparison of Ba/Ca_{foram} and bottom water Ba from sampling station M599

Here, we present our Ba/Ca_{foram} data in relation to the measured bottom water Ba/Ca from one of the investigated stations in the Northern Aegean Sea, in order to place our partition coefficients for *U. mediterranea* and *M. affinis* in the context of existing core top and laboratory calibrations for a range of (other) species. Station M599 is located in the Sporades Basin, which is connected and/or combined with

the Athos Basin to the Northeast (Fig. 1, Poulos, 2009). Selecting this station for the definition of a species-specific partition coefficient (representative at minimum for the Northern and Central Aegean seas) yields a first estimate about its magnitude. Since it has been shown that subsurface waters in the Aegean Sea are subject to mixing and low residence times with fast replenishment of intermediate and deep waters, the applicability of this local comparison of Ba/Ca and bottom water Ba to the entire region and beyond is certainly limited (Section 1.1, e.g., Androulidakis et al., 2012). It has to be pointed out that there are no regional gradients in Ba/Ca although productivity is subject to a S to N gradient (Section 3.2, Fig. 5, and Table 1).

The measured bottom water Ba/Ca of 5.3 µmol/mol (Table 4; based on Ba conc. of ~70 nmol/L) at station M599 agrees well with other measured bottom water Ba from the Eastern Mediterranean Sea GEO-TRACES cruise (Roy-Barman et al., 2019). Therefore, we are confident that this value adequately represents the bottom water conditions at the time of sampling (the samples for foraminifera were taken in December 2001 at station M599 whereas seawater samples were taken at exactly the same location in December 2017).

The Ba/Ca of *M. affinis* is significantly higher in live and dead specimens compared to Ba/Ca of *U. mediterranea* for the data set as a whole (Fig. 2). Also, when subsampling for Ba/Ca from station M599 it became apparent that Ba/Ca of *M. affinis* is slightly elevated compared to *U. mediterranea* for all sampling depths within the sediment surface (Table 2, Fig. 7). In consequence, the difference in Ba/Ca between the two species leads to species-specific partition coefficients when calibrated against the same bottom water value of Ba/Ca (Fig. 10). For station M599 we calculate an average $D_{Ba}$ for *U. mediterranea* of 0.34 ($n = 55$ single spot measurements, see Table 2; associated Ba/Ca_{foram} RSD of 27 %) whereas $D_{Ba}$ of *M. affinis* is 0.49 ($n = 22$ single spot measurements, see Table 2; associated Ba/Ca_{foram} RSD of 34 %). In fact, $D_{Ba}$s are based on median values for Ba/Ca data from live and dead specimens combined, estimated live and dead differences in $D_{Ba}$ are shown in Fig. 10. We argue that it is valid for our data to combine live and dead Ba/Ca for the calculation of $D_{Ba}$ because we have shown that for both species there are no significant differences for the live vs. dead
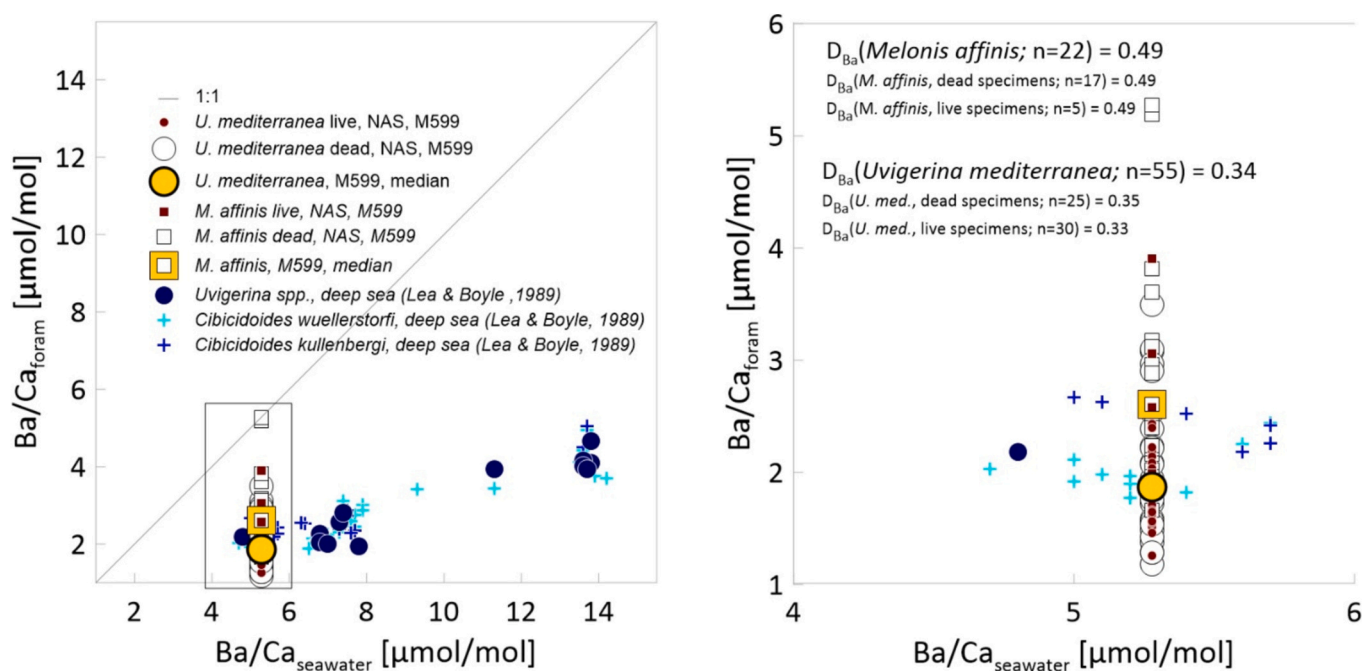


**Fig. 10.** Left: Ba/Ca_{foram} of all analysed specimens from station M599 in comparison to bottom water Ba/Ca measured at the same station (from samples of cruise M144). Also shown is the core top calibration of Ba/Ca_{foram} of Lea and Boyle (1989) for specimens of *Uvigerina* spp. and *C. wuellerstorfi,* as well as *C. kullenbergi* (orig. name; accepted name is *C. mundulus;* Brady, Parker & Jones, 1888; Hayward et al., 2023). Right: magnification of Ba/Ca range measured in this study with species-specific partition coefficients shown in legend.

comparison (if certain high values are excluded for *M. affinis*, Section 3.1). This similarity in dead and live Ba/Ca indicates that the dead fauna (in general, but specifically at station M599) has not undergone substantial transport or redeposition. For assessing the age of our dead specimens, we use sedimentation rates calculated from upper sections of cores from the Athos and Sporades basins, which show a range of 15–17 cm/ka (Kuhnt et al., 2007; Giamali et al., 2019; note that the latter authors also estimated sedimentation rates of 43 cm/ka for a core from the Athos Basin). It seems reasonable to estimate the age of our dead specimens at this station to be several hundred years at maximum, following similar age assessments for specimens from the same sites and sampling campaign as presented by Theodor et al. (2016a). Moreover, Theodor et al. (2016a) suggest that in selecting live and dead specimens from the same sediment depth, age differences should be minor, and that also effects of redeposition and bioturbation can be excluded for station M599. Therefore, it is valid to combine Ba/Ca of our live and dead specimens in order to calculate $D_{Ba}$ for the total fauna.

In comparison to $D_{Ba}$ found by other core top studies, we find similar values in the same order of magnitude (Table 5). It is striking that our $D_{Ba}$ for *U. mediterranea* is matching exactly the $D_{Ba}$ of *Uvigerina* spp. from surface sediments in deep-sea settings (water depths 830–5000 m; Lea and Boyle, 1989). This observation also suggests that to a certain extent laser ablation ICP-MS yields comparable data to solution ICP-MS (used by Lea and Boyle, 1989). The $D_{Ba}$ of *M. affinis* (0.49) is at the upper end of reported values, and is remarkably closely comparable to the value of coastal benthic species ($D_{Ba}$ of 0.57 ± 0.02) for a measured bottom water Ba of 19.49 μmol/mol (Groeneveld et al., 2018), which is substantially higher than our bottom water Ba of 5.3 μmol/mol. This similarity in $D_{Ba}$ might support our hypothesis 3 from Section 4.2.3 regarding the higher pore water Ba in the microhabitat of *M. affinis* compared to *U. mediterranea* leading to higher Ba/Ca for *M. affinis*. On the other hand, the relatively high $D_{Ba}$ of 0.5 ± 0.1 for epifaunal *C. pachyderma* from culturing experiments compared to lower $D_{Ba}$ for infaunal species from the same culturing experiments of Havach et al. (2001) does not support our hypothesis of higher $D_{Ba}$ for species with a

deeper microhabitat. It should be noted that the authors of the study suggest that pore water effects are an unlikely explanation for the observed differences in $D_{Ba}$ between species (Havach et al., 2001).

In comparison to $D_{Ba}$ from inorganic calcite ($D_{Ba\text{-}inorganic}$ = 0.01–0.06; as determined by growth experiments, e.g., Pingitore and Eastman, 1984; Tesoriero and Pankow, 1996) which is one order of magnitude lower than the $D_{Ba\text{-}foram}$, we can show that the Ba/Ca of our live and dead specimens seems to reflect a rather pristine signal of the primary foraminiferal calcite.

With our method, we can add interesting details regarding the variability across species and specimens from the same site (and thus the same bottom water Ba/Ca) as well as intra-test variability (discussed in Section 4.1). The range of Ba/Ca of *U. mediterranea* from station M599 is almost the same as the range of Ba/Ca of *Uvigerina* spp. from multiple core tops with Ba/Ca$_{seawater}$ reaching up to 14 μmol/mol (compared to the 5.3 μmol/mol at station M599, Table 5, Fig. 10). This high Ba/Ca$_{foram}$ range for single specimens of two different benthic species and a specific value of Ba/Ca$_{seawater}$ highlights once more that variability in Ba/Ca (and also other elements) may hold in itself important information about vital effects, ontogenetic trends, and species-specific incorporation of elements.

### 4.4. Global implications and directions of future research

For paleoceanographic applications, such as reconstructions of bottom water conditions and Ba cycling, with the ultimate goal of estimating export productivity, it is important to point out the limitations, presented here for the Northern and Central Aegean seas. The net export of Ba to bottom waters from surface waters may be related to export productivity. However, local differences and regional gradients in surface productivity, and or riverine input, reflected possibly by differences in Ba content of surface waters, may have been masked through formation and distribution of subsurface waters with low residence times (Zervakis et al., 2003; Pazi, 2008; Androulidakis et al., 2012).

Nevertheless, we have shown that it is possible to estimate bottom

**Table 5**

Summary of partition coefficients from this study and published data, with respective methodology and associated bottom water Ba/Ca (as well as environmental parameters, if available for deep-sea and shelf core tops).

|  | $D_{Ba}$ | Species | live/dead | Ba/Ca method | Ba/Ca$_{bw}$ (μmol/mol) | PP (g C/ m$^{-2}$a$^{-1}$) | C$_{org}$ (g C/ m$^{-2}$a$^{-1}$) | Study area | Water depth (m) | Authors |
|---|---|---|---|---|---|---|---|---|---|---|
| Deep-sea core top | 0.34 | *U. mediterranea* | live and dead | LA-ICP-MS | 5.3 | 195.88 | 8.66 | NAS | 1084 | this study |
|  | 0.49 | *M. affinis* | live and dead | LA-ICP-MS | 5.3 | 195.88 | 8.66 | NAS | 1084 | this study |
|  | 0.34 | *Uvigerina* spp. | dead | ID flow injection ICP-MS + flame atomic absorption (for Ca) | ~4.7–14.2 |  |  | Atlantic, Pacific, Indian oceans | 830–5000 | Lea and Boyle (1989) |
|  | 0.37–0.41 | *Cibicidoides* spp. | dead | ID flow injection ICP-MS + flame atomic absorption (for Ca) | ~4.7–14.2 |  |  | Atlantic, Pacific, Indian oceans | 830–5000 | Lea and Boyle (1989) |
| Shelf core top | 0.57 ± 0.02 | *Elphidium* spp. and *Ammonia* spp. | dead | ICP-OES | 19.49 | ~57.7[a] |  | Kattegat and Baltic Proper (Hanö Bay) | 10–70 | Groeneveld et al. (2018) |
| Cult. exper. | 0.33 | *A. lessonii* | live | LA-ICP-MS | 50–90 |  |  |  |  | de Nooijer et al. (2017) |
|  | 0.78 | *H. depressa* | live | LA-ICP-MS | 50–90 |  |  |  |  | de Nooijer et al. (2017) |
|  | 0.24 ± 0.06 | *U. peregrina* | live | ID ICP-MS | 55 ± 2 |  |  |  |  | Havach et al. (2001) |
|  | 0.5 ± 0.1 | *C. pachyderma* | live | ID ICP-MS | 55 ± 2 |  |  |  |  | Havach et al. (2001) |
|  | 0.24 ± 0.07 | *B. marginata* | live | ID ICP-MS | 55 ± 2 |  |  |  |  | Havach et al. (2001) |
|  | 0.20 ± 0.04 | *A. beccarii* | live | ID ICP-MS | 62 ± 2 |  |  |  |  | Havach et al. (2001) |

[a] For Bornholm Basin, Baltic Proper (Filipsson et al., 2017).

water Ba variability based on infaunal benthic foraminiferal Ba/Ca. Such applications may serve in deep-sea areas with less complex cycling of nutrients in bottom waters, and linkage to primary productivity, to assess variability in palaeo-export productivity. In order to place the results in a global context, it is important to characterise the Northern and Central Aegean seas in terms of productivity, and compare it to, e.g., open-ocean conditions. The presented primary productivity data for the study area were derived from satellite data prior to the year of sampling of the surface sediments. Theodor et al. (2016a) show that both PP and $C_{org}$ fluxes can be underestimated in these marginal basins (e.g., up to an order of magnitude when only considering the spring season) based on measurements from the water column. Therefore, we point out that, although being comparably lower than other ocean areas, $C_{org}$ fluxes in the Aegean Sea could in theory serve well to study the impact on Ba/Ca ratios of benthic foraminifera with potentially wider implications.

In Section 4.3 we have shown that our local partition coefficient for Ba/Ca of *U. mediterranea* is matching those values found by a global deep-sea calibration for *Uvigerina* spp. (Lea and Boyle, 1989). Therefore, our results strengthen the application of this $D_{Ba}$ for palaeoceanographic reconstructions using the genus *Uvigerina*, since also in marginal basins with sporadic ventilation events the calibration can confidently reconstruct bottom water Ba. We could speculate that the application of our $D_{Ba}$ to reconstruct past primary productivity would strengthen results of benthic foraminiferal faunal proxies. The latter are indicating higher seasonal marine organic matter fluxes (in the Northern Aegean Sea, for which we do not recommend the Ba/Ca$_{foram}$ proxy application, and) at coring sites in the Eastern Mediterranean Sea during deposition of sapropel S1 (~10.2–6.4 ka BP) compared to reconstructed most recent conditions (Schmiedl et al., 2010).

In order to suggest future directions of research on Ba/Ca calibration, we highlight once more one of the hypotheses addressed in this study. For further evaluation of the supposed microhabitat effects of the studied shallow and intermediate infaunal species (Section 4.2.3), additional species from other microhabitats should be included. Especially, Ba/Ca data from strictly epifaunal species would be useful to confirm microhabitat effects in infaunal species. An important aspect to strengthen such study designs is the availability of both *in situ* bottom and pore water Ba concentrations. Finally, in order to link the bottom water conditions to primary productivity, it is desirable to use samples originating from a study area in deep-sea settings with precise information on primary and export productivity.

## 5. Conclusions

Ba/Ca ratios of live (Rose Bengal stained) and dead specimens of *Uvigerina mediterranea* and *Melonis affinis* from surface sediments of seven stations within the Northern and Central Aegean seas have been analysed by LA-ICP-MS in order to better understand underlying processes of Ba incorporation into benthic foraminiferal tests. We observe a strong variability without specific trends related to measured environmental variables (e.g., primary productivity, and $C_{org}$ fluxes) of foraminiferal Ba/Ca for both analysed species between the different stations and basins in the study area. This observation likely reflects small-scale differences in Ba cycling between the stations. The distribution of nutrients and organic matter, and in turn Ba, in the deep basins of the Northern and Central Aegean seas may be difficult to characterise on short timescales. We point out the limitation of using Ba/Ca$_{foram}$ to reconstruct, and estimate palaeo-export productivity in these parts of the Aegean Sea, where on millennial time scales changes in riverine input/surface productivity, and stagnating bottom waters have led to the formation of sapropelic sediments.

Nevertheless, if we can transfer the fundamental insights on Ba incorporation to deep-sea areas with less complex and dynamic distribution of nutrients in bottom waters, the proxy application is strengthened by our findings that the Ba/Ca of dead foraminiferal specimens seems to be representative for the total fauna of both analysed species

which we assessed through comparison of data from live and dead specimens and their respective intra-test variability. From the comparison of Ba/Ca intra-test variability to other el/Ca from our specimens and to published values, it seems that most of the Ba/Ca intra-test variability of 16–24 % can be attributed to intrinsic factors, and more specifically vital effects during chamber growth, since consistent ontogenetic trends could not be observed. We discussed analytical aspects, biomineralisation processes, and ecological factors (species-specific microhabitat within the sediment surface of infaunal benthic foraminiferal species) as possible reasons to explain the observed significantly higher Ba/Ca of *M. affinis* compared to *U. mediterranea*. We can rule out biases due to the used analytical method of LA-ICP-MS, since scrutinizing and data reduction lead to the comparability of data from both species. However, it remains open if a single factor such as biomineralisation processes or the specific microhabitat related to early diagenetic processes within the surface sediment is responsible for the observed consistently increased Ba/Ca of *M. affinis* compared to *U. mediterranea* throughout most stations and sediment depths.

By comparing the Ba/Ca ratios of one particular station in the Northern Aegean Sea (M599) to seawater Ba/Ca measured from bottom water samples at the same site, we can suggest that species-specific partition coefficients are comparable to published $D_{Ba}$ from core tops and culturing experiments. We add valuable insights into possible reasons for the need of species-specific calibrations (see above), and show that live and dead specimens yield similar $D_{Ba}$, meaning that $D_{Ba-dead}$ is representative for the total fauna. The Ba/Ca intra-test variability, attributed to biomineralisation processes, can lead to a large scatter of $D_{Ba}$ from single chamber measurements (measured by LA-ICP-MS). We average the data of numerous analysed specimens of the same species for the comparison to Ba/Ca$_{seawater}$ to lay the foundation for calibrations in order to reconstruct bottom water conditions in deep-sea areas.

## CRediT authorship contribution statement

## Declaration of competing interest

The authors declare that they have no known competing financial interests or personal relationships that could have appeared to influence the work reported in this paper.

## Data availability

Ba/Ca, as well as Mg/Ca, Sr/Ca, and Na/Ca single chamber data are available through Mendeley Data at doi: 10.17632/cfbmyg67fv.2.

## Acknowledgements

## Appendix A. Supplementary data

Supplementary data to this article can be found online at https://doi.org/10.1016/j.marmicro.2024.102431.

## References

Abu-Zied, R.H., Rohling, E.J., Jorissen, F.J., Fontanier, C., Casford, J.S.L., Cooke, S., 2008. Benthic foraminiferal response to changes in bottom-water oxygenation and organic carbon flux in the eastern Mediterranean during LGM to recent times. Mar. Micropaleontol. 67, 46–68. https://doi.org/10.1016/j.marmicro.2007.08.006.

Aksu, A.E., Yaşar, D., Mudie, P.J., Gillespie, H., 1995. Late glacial-Holocene paleoclimatic and paleoceanographic evolution of the Aegean Sea: micropaleontological and stable isotopic evidence. Mar. Micropaleontol. 25, 1–28. https://doi.org/10.1016/0377-8398(94)00026-J.

Androulidakis, Y.S., Kourafalou, V.H., Krestenitis, Y.N., Zervakis, V., 2012. Variability of deep water mass characteristics in the North Aegean Sea: the role of lateral inputs and atmospheric conditions. Deep. Res. Part I Oceanogr. Res. Pap. 67, 55–72. https://doi.org/10.1016/j.dsr.2012.05.004.

Androulidakis, Y.S., Krestenitis, Y.N., Psarra, S., 2017. Coastal upwelling over the North Aegean Sea: Observations and simulations. Cont. Shelf Res. 149, 32–51. https://doi.org/10.1016/j.csr.2016.12.002.

Angus, J.G., Raynor, J.B., Robson, M., 1979. Reliability of experimental partition coefficients in carbonate systems: evidence for inhomogeneous distribution of impurity cations. Chem. Geol. 27, 181–205. https://doi.org/10.1016/0009-2541(79)90038-X.

Antoine, D., Morel, A., 1996. Oceanic primary production: 1. Adaptation of a spectral light-photosynthesis model in view of application to satellite chlorophyll observations. Global Biogeochem. Cy. 10, 43–55. https://doi.org/10.1029/95GB02831.

Barker, S., Greaves, M., Elderfield, H., 2003. A study of cleaning procedures used for foraminiferal Mg/Ca paleothermometry. Geochem. Geophys. Geosyst. 4, 8407. https://doi.org/10.1029/2003GC000559.

Barras, C., Mouret, A., Nardelli, M.P., Metzger, E., Petersen, J., La, C., Filipsson, H.L., Jorissen, F.J., 2018. Experimental calibration of manganese incorporation in foraminiferal calcite. Geochim. Cosmochim. Acta 237, 49–64.

Becker, J.J., Sandwell, D.T., Smith, W.H.F., Braud, J., Binder, B., Depner, J., Fabre, D., Factor, J., Ingalls, S., Kim, S.H., Ladner, R., Marks, K., Nelson, S., Pharaoh, A., Trimmer, R., von Rosenberg, J., Wallace, G., Weatherall, P., 2009. Global Bathymetry and Elevation Data at 30 Arc seconds Resolution: SRTM30_PLUS. Mar. Geod. 32, 355–371. https://doi.org/10.1080/01490410903297766.

Bentov, S., Erez, J., 2005. Novel observations on biomineralization processes in foraminifera and implications for Mg/Ca ratio in the shells. Geology 33, 841–844. https://doi.org/10.1130/G21800.1.

Bentov, S., Erez, J., 2006. Impact of biomineralization processes on the Mg content of foraminiferal shells: a biological perspective. Geochem. Geophys. Geosyst. 7, Q01P08. https://doi.org/10.1029/2005GC001015.

Bernhard, J.M., . Distinguishing Live from Dead Foraminifera : Methods Review and Proper Applications Author (s): Joan M. Bernhard Stable. http://www.jstor.org/stable/1486179. Distinguishing live from dead foraminifera : Methods review and proper applications. micropaleontolgy Proj. Inc, 46, pp. 38–46.

Betzer, P.R., Showers, W.J., Laws, E.A., Winn, C.D., DiTullio, G.R., Kroopnick, 1984. Primary productivity and particle fluxes on a transect of the equator at 153° W in the Pacific Ocean. Deep-Sea Res. 31, 1–11. https://doi.org/10.1016/0198-0149(84)90068-2.

Bishop, J.K.B., 1988. The barite-opal-organic carbon association in oceanic particulate matter. Nature 332, 341–343. https://doi.org/10.1038/332341a0.

Bozyiğit, C., Eriş, K.K., Sicre, M.A., Çağatay, M.N., Uçarkuş, G., Klein, V., Gasperini, L., 2022. Middle-late Holocene climate and hydrologic changes in the Gulf of Saros (NE Aegean Sea). Mar. Geol. 443. https://doi.org/10.1016/j.margeo.2021.106688.

Branson, O., Bonnin, E.A., Perea, D.E., Spero, H.J., Zhu, Z., Winters, M., Hönisch, B., Russell, A.D., Fehrenbacher, J.S., Gagnon, A.C., 2016. Nanometer-Scale Chemistry of a Calcite Biomineralization Template: Implications for Skeletal Composition and Nucleation. Proc. Natl. Acad. Sci. USA 113, 12934–12939. https://doi.org/10.1073/pnas.1522864113.

Brinkmann, I., Barras, C., Jilbert, T., Næraa, T., Paul, K.M., Schweizer, M., Filipsson, H.L., 2022. Drought recorded by Ba/Ca in coastal benthic foraminifera. Biogeosciences 19, 2523–2535. https://doi.org/10.5194/bg-19-2523-2022.

Carter, S.C., Paytan, A., Griffith, E.M., 2020. Toward an improved understanding of the marine barium cycle and the application of marine barite as a paleoproductivity proxy. Minerals 10, 1–24. https://doi.org/10.3390/min10050421.

Casford, J.S.L., Rohling, E.J., Abu-Zied, R.H., Fontanier, C., Jorissen, F.J., Leng, M.J., Schmiedl, G., Thomson, J., 2003. A dynamic concept for eastern Mediterranean circulation and oxygenation during sapropel formation. Palaeogeogr. Palaeoclimatol. Palaeoecol. 190, 103–119. https://doi.org/10.1016/S0031-0182(02)00601-6.

Caulle, C., Koho, K.A., Mojtahid, M., Reichart, G.J., Jorissen, F.J., 2014. Live (Rose Bengal stained) foraminiferal faunas from the northern Arabian Sea: Faunal succession within and below the OMZ. Biogeosciences 11, 1155–1175. https://doi.org/10.5194/bg-11-1155-2014.

Church, T.M., Wolgemuth, K., 1972. Marine barite saturation. Earth Planet. Sci. Lett. 15, 35–44.

Curry, W.B., Marchitto, T.M., 2008. A secondary ionization mass spectrometry calibration of Cibicidoides pachyderma Mg/Ca with temperature. Geochem. Geophys. Geosyst. 9, Q04009. https://doi.org/10.1029/2007GC001620.

de Nooijer, L.J., Hathorne, E.C., Reichart, G.J., Langer, G., Bijma, J., 2014a. Variability in calcitic Mg/Ca and Sr/Ca ratios in clones of the benthic foraminifer Ammonia tepida. Mar. Micropaleontol. 107, 32–43. https://doi.org/10.1016/j.marmicro.2014.02.002.

de Nooijer, L.J., Spero, H.J., Erez, J., Bijma, J., Reichart, G.J., 2014b. Biomineralization in perforate foraminifera. Earth-Sci. Rev. 135, 48–58. https://doi.org/10.1016/j.earscirev.2014.03.013.

de Nooijer, L.J., Brombacher, A., Mewes, A., Langer, G., Nehrke, G., Bijma, J., 2017. Ba incorporation in benthic foraminifera. Biogeosciences 14, 3387–3400.

Dehairs, F., Fagel, N., Antia, A.N., Peinert, R., Elskens, M., Goeyens, L., 2000. Export production in the Bay of Biscay as estimated from barium - a comparison with new production. Deep. Res. Part I Oceanogr. Res. Pap. 47, 583–601. https://doi.org/10.1016/S0967-0637(99)00072-2.

Dickens, G.R., Fewless, T., Thomas, E., Bralower, T.J., 2003. Excess barite accumulation during the Paleocene-Eocene thermal Maximum: Massive input of dissolved barium from seafloor gas hydrate reservoirs. In: Causes and Consequences of Globally Warm Climates in the Early Paleogene, Volume 369. Geological Society of America, Boulder, CO, USA, pp. 11–23.

Dymond, J., Collier, R., 1996. Particulate barium fluxes and their relationships to biological productivity. Deep. Res. Part II Top. Stud. Oceanogr. 43, 1283–1308. https://doi.org/10.1016/0967-0645(96)00011-2.

Filipsson, H.L., McCorkle, D.C., Mackensen, A., Bernhard, J.M., Andersson, L.S., Naustvoll, L.J., Caballero-Alfonso, A.M., Nordberg, K., Danielssen, D.S., 2017. Seasonal variability of stable carbon isotopes (δ13CDIC) in the Skagerrak and the Baltic Sea: Distinguishing between mixing and biological productivity. Palaeogeogr. Palaeoclimatol. Palaeoecol. 483, 15–30. https://doi.org/10.1016/j.palaeo.2016.11.031.

Fontanier, C., Jorissen, F.J., Licari, L., Alexandre, A., Anschutz, P., Carbonel, P., 2002. Live benthic foraminiferal faunas from the Bay of Biscay: faunal density, composition, and microhabitats. Deep-Sea Res. I Oceanogr. Res. Pap. 49, 751–785.

Geslin, E., Heinz, P., Jorissen, F., Hemleben, C., 2004. Migratory responses of deep-sea benthic foraminifera to variable oxygen conditions: Laboratory investigations. Mar. Micropaleontol. 53, 227–243. https://doi.org/10.1016/j.marmicro.2004.05.010.

Geslin, E., Barras, C., Langlet, D., Nardelli, M.P., Kim, J.-H., Bonnin, J., Metzger, E., Jorissen, F.J., 2014. Survival, reproduction and calcification of three benthic foraminiferal species in response to experimentally induced hypoxia. In: Kitazato, H., Bernhard, J.M. (Eds.), Approaches to Study Living Foraminifera: Collection, Maintenance and Experimentation. Springer, Japan, pp. 163–193. https://doi.org/10.1007/978-4-431-54388-6.

Giamali, C., Koskeridou, E., Antonarakou, A., Ioakim, C., Kontakiotis, G., Karageorgis, A. P., Roussakis, G., Karakitsios, V., 2019. Multiproxy ecosystem response of abrupt holocene climatic changes in the northeastern Mediterranean sedimentary archive and hydrologic regime. Quat. Res. (United States) 92, 1–21. https://doi.org/10.1017/qua.2019.38.

Glock, N., Eisenhauer, A., Liebetrau, V., Wiedenbeck, M., Hensen, C., Nehrke, G., 2012. EMP and SIMS studies on Mn/Ca and Fe/Ca systematics in benthic foraminifera from the Peruvian OMZ: a contribution to the identification of potential redox proxies and the impact of cleaning protocols. Biogeosciences 9, 341–359. https://doi.org/10.5194/bg-9-341-2012.

Glock, N., Liebetrau, V., Eisenhauer, A., Rocholl, A., 2016. High resolution I/Ca ratios of benthic foraminifera from the Peruvian oxygen-minimum-zone: a SIMS derived assessment of a potential redox proxy. Chem. Geol. 447, 40–53. https://doi.org/10.1016/j.chemgeo.2016.10.025.

Groeneveld, J., Filipsson, H.L., Austin, W.E.N., Darling, K., McCarthy, D., Krupinski, N.B. Q., Bird, C., Schweizer, M., 2018. Assessing proxy signatures of temperature, salinity, and hypoxia in the Baltic Sea through foraminifera-based geochemistry and faunal assemblages. J. Micropalaeontol. 37, 403–429. https://doi.org/10.5194/jm-37-403-2018.

Guo, X., Xu, B., Burnett, W.C., Yu, Z., Yang, S., Huang, X., Wang, F., Nan, H., Yao, P., Sun, F., 2019. A potential proxy for seasonal hypoxia: LA-ICP-MS Mn/Ca ratios in benthic foraminifera from the Yangtze River Estuary. Geochim. Cosmochim. Acta 245, 290–303. https://doi.org/10.1016/j.gca.2018.11.007.

Guo, X., Yuan, H., Burnett, W., Zhang, H., Lian, E., Xu, H., Yu, Z., Xu, B., 2023. Ba/Ca in foraminifera shells as a proxy of submarine groundwater discharge. Limnol. Oceanogr. Lett. 8, 490–497. https://doi.org/10.1002/lol2.10290.

Guo, X., Lian, E., Yuan, H., Burnett, W.C., Zhang, H., Zhang, M., Xiao, K., Wei, Q., Yu, Z., Xu, B., 2024. Proxies of hypoxia and submarine groundwater discharge in the coastal ocean: Foraminiferal shell chemical perspectives. Mar. Chem. 265–266, 104434. https://doi.org/10.1016/j.marchem.2024.104434.

Havach, S.M., Chandler, G.T., Wilson-Finelli, A., Shaw, T.J., 2001. Experimental determination of trace element partition coefficients in cultured benthic foraminifera. Geochim. Cosmochim. Acta 65, 1277–1283. https://doi.org/10.1016/S0016-7037(00)00563-9.

Hayward, B.W., Le Coze, F., Vachard, D., Gross, O., 2023. World Foraminifera Database. *Cibicidoides kullenbergi* (Parker, 1953) [WWW Document]. World Regist. Mar. Species. https://www.marinespecies.org/aphia.php?p=taxdetails&id=112883 (on 2023-05-31).

Hemleben, C., Hoernle, K., Jørgensen, B.B., Roether, W. (Eds.), 2001. Ostatlantik - Mittelmeer - Schwarzes Meer, Cruise No. 51, 12 September – 28 December 2001. METEOR-Berichte, Univ. Hambg, 03–1 (225 pp).

Higgs, N.C., Thomson, J., Wilson, T.R.S., Croudace, I.W., 1994. Modification and complete removal of eastern Mediterranean sapropels by postdepositional oxidation. Geology 22, 423–426. https://doi.org/10.1130/0091-7613(1994)022<0423:MACROE>2.3.CO;2.

Hoogakker, B.A.A., Elderfield, H., Schmiedl, G., Mccave, I.N., Rickaby, R.E.M., 2015. Glacial – Interglacial Changes in Bottom-Water Oxygen Content on the Portuguese Margin, 8, pp. 2–5. https://doi.org/10.1038/NGEO2317.

Jaccard, S.L., Hayes, C.T., Martínez-García, A., Hodell, D.A., Anderson, R.F., Sigman, D. M., Haug, G.H., 2013. Two modes of change in Southern Ocean productivity over the past million years. Science (80-.) 339, 1419–1423. https://doi.org/10.1126/science.1227545.

Jochum, K.P., Scholz, D., Stoll, B., Weis, U., Wilson, S.A., Yang, Q., Schwalb, A., Börner, N., Jacob, D.E., Andreae, M.O., 2012. Accurate trace element analysis of speleothems and biogenic calcium carbonates by LA-ICP-MS. Chem. Geol. 318–319, 31–44. https://doi.org/10.1016/j.chemgeo.2012.05.009.

Jochum, K.P., Garbe-Schönberg, D., Veter, M., Stoll, B., Weis, U., Weber, M., Lugli, F., Jentzen, A., Schiebel, R., Wassenburg, J.A., Jacob, D.E., Haug, G.H., 2019. Nano-powdered calcium carbonate reference materials: significant progress for microanalysis? Geostand. Geoanal. Res. 43, 595–609. https://doi.org/10.1111/ggr.12292.

Jorissen, F.J., 2003. Benthic foraminiferal microhabitats below the sediment-water interface. In: Sen Gupta, B.K. (Ed.), Modern Foraminifera. Kluwer Academic Publishers, pp. 161–180.

Jorissen, F.J., de Stigter, H., Widmark, J.G.V., 1995. A conceptual model explaining benthic foraminiferal microhabitats. Mar. Micropaleontol. 26, 3–15.

Kitano, Y., Kanamori, N., Oomori, T., 1971. Measurements of distribution coefficients of strontium and barium between carbonate precipitate and solution - Abnormally high values of distribution coefficients measured at early stages of carbonate formation. Geochem. J. 4.

Koho, K.A., García, R., de Stigter, H.C., Epping, E., Koning, E., Kouwenhoven, T.J., van der Zwaan, G.J., 2008. Sedimentary labile organic carbon and pore water redox control on species distribution of benthic foraminifera: a case study from Lisbon-Setúbal Canyon (southern Portugal). Prog. Oceanogr. 79, 55–82. https://doi.org/10.1016/j.pocean.2008.07.004.

Koho, K.A., de Nooijer, L.J., Reichart, G.J., 2015. Combining benthic foraminiferal ecology and shell Mn/Ca to deconvolve past bottom water oxygenation and paleoproductivity. Geochim. Cosmochim. Acta 165, 294–306. https://doi.org/10.1016/j.gca.2015.06.003.

Kuhnt, T., Schmiedl, G., Ehrmann, W., Hamann, Y., Hemleben, C., 2007. Deep-sea ecosystem variability of the Aegean Sea during the past 22 kyr as revealed by Benthic Foraminifera. Mar. Micropaleontol. 64, 141–162. https://doi.org/10.1016/j.marmicro.2007.04.003.

Langer, G., Sadekov, A., Thoms, S., Keul, N., Nehrke, G., Mewes, A., Greaves, M., Misra, S., Reichart, G., Jan, L., Nooijer, D., Bijma, J., Elder, H., 2016. Sr Partitioning in the Benthic Foraminifera *Ammonia aomoriensis* and *Amphistegina lessonii*, 440, pp. 306–312. https://doi.org/10.1016/j.chemgeo.2016.07.018.

Le Houedec, S., Mojtahid, M., Bicchi, E., de Lange, G.J., Hennekam, R., 2020. Suborbital hydrological variability inferred from coupled Benthic and Planktic Foraminiferal-based proxies in the Southeastern Mediterranean during the past 19 ka. Paleoceanogr. Paleoclimatol. 35, 1–23. https://doi.org/10.1029/2019PA003827.

Lea, D.W., 1993. Constraints on the alkalinity and circulation of glacial circumpolar deep water from benthic foraminiferal barium. Glob. Biogeochem. Cycles 7, 695–710.

Lea, D.W., Boyle, E., 1989. Barium content of benthic foraminifera cotrolled by bottom-water composition. Nature 338, 751–753.

Lea, D.W., Spero, H.J., 1992. Experimental determination of barium uptake in shells of the planktonic foraminifera *Orbulina universa* at 22°C. Geochim. Cosmochim. Acta 56, 2673–2680. https://doi.org/10.1016/0016-7037(92)90352-J.

Leduc, M., Garbe-Schönberg, D., Regenberg, M., Contoux, C., Etourneau, J., Schneider, R., 2014. The late Pliocene Benguela upwelling status revisited by means of multiple temperature proxies. Geochem. Geophys. Geosyst. 15, 475–491. https://doi.org/10.1002/2013GC004940.

Licari, L.N., Schumacher, S., Wenzhöfer, F., Zabel, M., Mackensen, A., 2003. Communities and microhabitats of living benthic foraminifera from the tropical East Atlantic: Impact of different productivity regimes. J. Foraminifer. Res. 33, 10–31. https://doi.org/10.2113/0330010.

Lorens, R.B., 1981. Sr, Cd, Mn and Co distribution coefficients in calcite as a function of calcite precipitation rate. Geochim. Cosmochim. Acta 45, 553–561. https://doi.org/10.1016/0016-7037(81)90188-5.

Lutze, G.F., Altenbach, A., 1991. Technique for Staining living Benthic Foraminfera with Rose Bengal. Geol. Jahrb. A 128, 251–265.

Lykousis, V., Chronis, G., Tselepides, A., Price, N.B., Theocharis, A., Siokou-Frangou, I., Van Wambeke, F., Danovaro, R., Stavrakakis, S., Duineveld, G., Georgopoulos, D., Ignatiades, L., Souvermezoglou, A., Voutsinou-Taliadouri, F., 2002. Major outputs of the recent multidisciplinary biogeochemical researches undertaken in the Aegean Sea. J. Mar. Syst. 33–34, 313–334. https://doi.org/10.1016/S0924-7963(02)00064-7.

Lynch-Stieglitz, J., Vollmer, T.D., Valley, S.G., Blackmon, E., Gu, S., Marchitto, T.M., 2024. A diminished North Atlantic nutrient stream during Younger Dryas climate reversal. Science (80-.) 384, 693–696. https://doi.org/10.1126/science.adi5543.

Marr, J.P., Baker, J.A., Carter, L., Allan, A.S.R., Dunbar, G.B., Bostock, H.C., 2011. Ecological and temperature controls on Mg/Ca ratios of *Globigerina bulloides* from the Southwest Pacific Ocean. Paleoceanography 26, PA2209. https://doi.org/10.1029/2010PA002059.

McCorkle, D.C., Martin, P.A., Lea, D.W., Klinkhammer, G.P., 1995. Evidence of a dissolution effect on benthic foraminiferal shell chemistry : $\delta^{13}C$, Cd / Ca, Ba / Ca, and Sr / Ca results from the Ontong Java Plateau. Paleoceanography 10, 699–714.

McCorkle, D.C., Corliss, B.H., Farnham, C.A., 1997. Vertical distribution and stable isotopic compostition of live (stained) Benthic Foraminifera from the North Carolina and California margins. Deep. Res. Part I 44, 983–1024.

McManus, J., Berelson, W.M., Klinkhammer, G.P., Johnson, K.S., Coale, K.H., Anderson, R.F., Kumar, N., Burdige, D.J., Hammond, D.E., Brumsack, H.J., McCorkle, D.C., Rushdi, A., 1998. Geochemistry of barium in marine sediments: implications for its use as a paleoproxy. Geochim. Cosmochim. Acta 62, 3453–3473. https://doi.org/10.1016/S0016-7037(98)00248-8.

MedAtlas, 1997. Mediterranean Hydrographic Atlas (Mast Supporting Initiative; MAS2-CT93-0074) p. CD-ROM.

Mezger, E.M., de Nooijer, L.J., Siccha, M., Brummer, G.J.A., Kucera, M., Reichart, G.J., 2018. Taphonomic and Ontogenetic Effects on Na/Ca and Mg/Ca in Spinose Planktonic Foraminifera from the Red Sea. Geochem. Geophys. Geosyst. 19, 4174–4194. https://doi.org/10.1029/2018GC007852.

Möbius, J., Lahajnar, N., Emeis, K.C., 2010. Diagenetic control of nitrogen isotope ratios in Holocene sapropels and recent sediments from the Eastern Mediterranean Sea. Biogeosciences 7, 3901–3914. https://doi.org/10.5194/bg-7-3901-2010.

Mojtahid, M., Griveaud, C., Fontanier, C., Anschutz, P., Jorissen, F.J., 2010. Live benthic foraminiferal faunas along a bathymetrical transect (140–4800m) in the Bay of Biscay (NE Atlantic). Rev. Micropaléontol. 53, 139–162. https://doi.org/10.1016/j.revmic.2010.01.002.

Mojtahid, M., Hennekam, R., De Nooijer, L., Reichart, G.J., Jorissen, F., Boer, W., Le Houedec, S., De Lange, G.J., 2019. Evaluation and application of foraminiferal element/calcium ratios: Assessing riverine fluxes and environmental conditions during sapropel S1 in the Southeastern Mediterranean. Mar. Micropaleontol. 153. https://doi.org/10.1016/j.marmicro.2019.101783.

Moller, T., Schulz, H., Hamann, Y., Dellwig, O., Kucera, M., 2012. Sedimentology and geochemistry of an exceptionally preserved last interglacial sapropel S5 in the Levantine Basin (Mediterranean Sea). Mar. Geol. 291–294, 34–48. https://doi.org/10.1016/j.margeo.2011.10.011.

Nagai, Y., Uematsu, K., Chen, C., Wani, R., Tyszka, J., Toyofuku, T., 2018. Weaving of biomineralization framework in rotaliid foraminifera: Implications for paleoceanographic proxies. Biogeosciences 15, 6773–6789. https://doi.org/10.5194/bg-15-6773-2018.

Nairn, M.G., Lear, C.H., Sosdian, S.M., Bailey, T.R., Beavington-Penney, S., 2021. Tropical Sea surface temperatures following the Middle Miocene climate transition from Laser-Ablation ICP-MS analysis of glassy foraminifera. Paleoceanogr. Paleoclimatol. 1–21. https://doi.org/10.1029/2020pa004165.

Nehrke, G., Langer, G., 2023. Proxy archives based on marine calcifying organisms and the role of process-based biomineralization concepts. Minerals 13, 1–12. https://doi.org/10.3390/min13040561.

Nehrke, G., Keul, N., Langer, G., De Nooijer, L.J., Bijma, J., Meibom, A., 2013. A new model for biomineralization and trace-element signatures of Foraminifera tests. Biogeosciences 10, 6759–6767. https://doi.org/10.5194/bg-10-6759-2013.

Ní Fhlaithearta, S., Reichart, G.J., Jorissen, F.J., Fontanier, C., Rohling, E.J., Thomson, J., De Lange, G.J., 2010. Reconstructing the seafloor environment during sapropel formation using benthic foraminiferal trace metals, stable isotopes, and sediment composition. Paleoceanography 25, PA4225. https://doi.org/10.1029/2009PA001869.

Ni, S., Quintana Krupinski, N.B., Groeneveld, J., Fanget, A.S., Böttcher, M.E., Liu, B., Lipka, M., Knudsen, K.L., Naeraa, T., Seidenkrantz, M.S., Filipsson, H.L., 2020. Holocene hydrographic variations from the Baltic-North Sea transitional area (IODP Site M0059). Paleoceanography. https://doi.org/10.1029/2019PA003722.

Paytan, A., Kastner, M., 1996. Benthic Ba fluxes in the central pacific, implications for the oceanic Ba cycle. Earth Planet. Sci. Lett. 142, 439–450.

Pazi, I., 2008. Water mass properties and chemical characteristics in the Saros Gulf, Northeast Aegean Sea (Eastern Mediterranean). J. Mar. Syst. 74, 698–710. https://doi.org/10.1016/j.jmarsys.2008.07.002.

Petersen, J., 2017. PhD Thesis: Development of Paleo-Oxygenation Proxies: New Insights into Mn/Ca and Pore Patterns of Benthic Foraminiferal Tests. Laboratory of Recent and Fossil Bioindicators. University of Nantes, Université Bretagne Loire.

Petersen, J., Barras, C., Bézos, A., La, C., De Nooijer, L.J., Meysman, F.J.R., Mouret, A., Slomp, C.P., Jorissen, F.J., 2018. Mn/Ca intra- and inter-test variability in the benthic foraminifer *Ammonia tepida*. Biogeosciences 15, 331–348. https://doi.org/10.5194/bg-15-331-2018.

Petersen, J., Barras, C., Bézos, A., La, C., Slomp, C.P., Meysman, F.J.R., Mouret, A., Jorissen, F.J., 2019. Mn/Ca ratios of *Ammonia tepida* as a proxy for seasonal coastal hypoxia. Chem. Geol. 518, 55–66. https://doi.org/10.1016/j.chemgeo.2019.04.002.

Pingitore, N.E., 1986. Modes of Coprecipitation of $Ba^{2+}$ and $Sr^{2+}$ with Calcite. In: DAVIS, J.F., HAYES, K.F. (Ed.), Geochemical Processes at Mineral Surfaces. American Chemical Society, pp. 574–586.

Pingitore, N.E., Eastman, M.P., 1984. The experimental partitioning of $Ba^{2+}$ into calcite. Chem. Geol. 45, 113–120.

Poulos, S.E., 2009. Origin and distribution of the terrigenous component of the unconsolidated surface sediment of the Aegean floor: a synthesis. Cont. Shelf Res. 29, 2045–2060. https://doi.org/10.1016/j.csr.2008.11.010.

Pross, J., Bahr, A., et al., 2021. M144-Eastern Mediterranean Paleoclimate and Ecosystems during the Rise of Early Civilizations. METEOR-Berichte, Univ. Hambg, Berichte.

R Core Team, 2016. R: A Language and Environment for Statistical Computing. R Foundation for Statistical Computing, Vienna, Austria.

Reichart, G.J., Jorissen, F., Anschutz, P., Mason, P.R.D., 2003. Single foraminiferal test chemistry records the marine environment. Geology 31, 355–358. https://doi.org/10.1130/0091-7613(2003)031<0355:SFTCRT>2.0.CO;2.

Richey, J.N., Fehrenbacher, J.S., Reynolds, C.E., Davis, C.V., Spero, H.J., 2022. Barium enrichment in the non-spinose planktic foraminifer, *Globorotalia truncatulinoides*. Geochim. Cosmochim. Acta 333, 184–199. https://doi.org/10.1016/j.gca.2022.07.006.

Roether, W., Klein, B., Manca, B.B., Theocharis, A., Kioroglou, S., 2007. Transient Eastern Mediterranean deep waters in response to the massive dense-water output of the Aegean Sea in the 1990s. Prog. Oceanogr. 74, 540–571. https://doi.org/10.1016/j.pocean.2007.03.001.

Rohling, E.J., Marino, G., Grant, K.M., 2015. Mediterranean climate and oceanography, and the periodic development of anoxic events (sapropels). Earth-Sci. Rev. 143, 62–97. https://doi.org/10.1016/j.earscirev.2015.01.008.

Roy-Barman, M., Pons-Branchu, E., Levier, M., Bordier, L., Foliot, L., Gdaniec, S., Ayrault, S., Garcia-Orellana, J., Masque, P., Castrillejo, M., 2019. Barium during the GEOTRACES GA-04S MedSeA cruise: the Mediterranean Sea Ba budget revisited. Chem. Geol. 511, 431–440. https://doi.org/10.1016/j.chemgeo.2018.09.015.

Schenau, S.J., Prins, M.A., De Lange, G.J., Monnin, C., 2001. Barium accumulation in the Arabian Sea: Controls on barite preservation in marine sediments. Geochim. Cosmochim. Acta 65, 1545–1556. https://doi.org/10.1016/S0016-7037(01)00547-6.

Schmiedl, G., Mackensen, A., 2006. Multispecies stable isotopes of benthic foraminifers reveal past changes of organic matter decomposition and deepwater oxygenation in the Arabian Sea. Paleoceanography 21, 1–14. https://doi.org/10.1029/2006PA001284.

Schmiedl, G., Pfeilsticker, M., Hemleben, C., Mackensen, A., 2004. Environmental and biological effects on the stable isotope composition of recent deep-sea benthic foraminifera from the western Mediterranean Sea. Mar. Micropaleontol. 51, 129–152. https://doi.org/10.1016/j.marmicro.2003.10.001.

Schmiedl, G., Kuhnt, T., Ehrmann, W., Emeis, K.C., Hamann, Y., Kotthoff, U., Dulski, P., Pross, J., 2010. Climatic forcing of eastern Mediterranean deep-water formation and benthic ecosystems during the past 22 000 years. Quat. Sci. Rev. 29, 3006–3020. https://doi.org/10.1016/j.quascirev.2010.07.002.

Skliris, N., Mantziafou, A., Sofianos, S., Gkanasos, A., 2010. Satellite-derived variability of the Aegean Sea ecohydrodynamics. Cont. Shelf Res. 30, 403–418. https://doi.org/10.1016/j.csr.2009.12.012.

Sperling, M., Schmiedl, G., Hemleben, C., Emeis, K.C., Erlenkeuser, H., Grootes, P.M., 2003. Black Sea impact on the formation of eastern Mediterranean sapropel S1? Evidence from the Marmara Sea. Palaeogeogr. Palaeoclimatol. Palaeoecol. 190, 9–21. https://doi.org/10.1016/S0031-0182(02)00596-5.

Spero, H.J., Eggins, S.M., Russell, A.D., Vetter, L., Kilburn, M.R., Hönisch, B., 2015. Timing and mechanism for intratest Mg/Ca variability in a living planktic foraminifer. Earth Planet. Sci. Lett. 409, 32–42. https://doi.org/10.1016/j.epsl.2014.10.030.

Tachikawa, K., Elderfield, H., 2002. Microhabitat effects on Cd/Ca and $\delta^{13}C$ of benthic foraminifera. Earth Planet. Sci. Lett. 202, 607–624. https://doi.org/10.1016/S0012-821X(02)00796-3.

Tachikawa, K., Vidal, L., Cornuault, M., Garcia, M., Pothin, A., Sonzogni, C., Bard, E., Menot, G., Revel, M., 2015. Eastern Mediterranean Sea circulation inferred from the conditions of S1 sapropel deposition. Clim. Past 11, 855–867. https://doi.org/10.5194/cp-11-855-2015.

Tesoriero, A.J., Pankow, J.F., 1996. Solid solution partitioning of $Sr^{2+}$, $Ba^{2+}$, and $Cd^{2+}$ to calcite. Geochim. Cosmochim. Acta 60, 1053–1063.

Theodor, M., Schmiedl, G., Jorissen, F., Mackensen, A., 2016a. Stable carbon isotope gradients in benthic foraminifera as proxy for organic carbon fluxes in the Mediterranean Sea. Biogeosciences 13, 6385–6404. https://doi.org/10.5194/bg-13-6385-2016.

Theodor, M., Schmiedl, G., Mackensen, A., 2016b. Stable isotope composition of deep-sea benthic foraminifera under contrasting trophic conditions in the western Mediterranean Sea. Mar. Micropaleontol. 124, 16–28. https://doi.org/10.1016/j.marmicro.2016.02.001.

Thomson, J., Higgs, N.C., Wilson, T.R.S., Croudace, I.W., De Lange, G.J., Van Santvoort, P.J.M., 1995. Redistribution and geochemical behaviour of redox-sensitive elements around S1, the most recent eastern Mediterranean sapropel. Geochim. Cosmochim. Acta 59, 3487–3501. https://doi.org/10.1016/0016-7037(95)00232-O.

Thomson, J., Croudace, I.W., Rothwell, R.G., 2006. A geochemical application of the ITRAX scanner to a sediment core containing eastern Mediterranean sapropel units. Geol. Soc. Spec. Publ. 267, 65–77. https://doi.org/10.1144/GSL.SP.2006.267.01.05.

Triantaphyllou, M.V., Gogou, A., Dimiza, M.D., Kostopoulou, S., Parinos, C., Roussakis, G., Geraga, M., Bouloubassi, I., Fleitmann, D., Zervakis, V., Velaoras, D., Diamantopoulou, A., Sampatakaki, A., Lykousis, V., 2016. Holocene Climatic Optimum centennial-scale paleoceanography in the NE Aegean (Mediterranean Sea). Geo-Marine Lett. 36, 51–66. https://doi.org/10.1007/s00367-015-0426-2.

Tsiaras, K.P., Kourafalou, V.H., Raitsos, D.E., Triantafyllou, G., Petihakis, G., Korres, G., 2012. Inter-annual productivity variability in the North Aegean Sea: Influence of thermohaline circulation during the Eastern Mediterranean Transient. J. Mar. Syst. 96–97, 72–81. https://doi.org/10.1016/j.jmarsys.2012.02.003.

Van der Zwaan, G.J., Duijnstee, I.A.P., den Dulk, M., Ernst, S.R., Jannink, N.T., Kouwenhoven, T.J., 1999. Benthic foraminifers : proxies or problems ? A review of paleoecological concepts. Earth-Sci. Rev. 46, 213–236.

van Dijk, I., Mouret, A., Cotte, M., Le Houedec, S., Oron, S., Reichart, G.J., Reyes-Herrera, J., Filipsson, H.L., Barras, C., 2019. Chemical Heterogeneity of Mg, Mn, Na, S, and Sr in Benthic Foraminiferal Calcite. Front. Earth Sci. 7, 1–23. https://doi.org/10.3389/feart.2019.00281.

Velaoras, D., Lascaratos, A., 2005. Deep water mass characteristics and interannual variability in the North and Central Aegean Sea. J. Mar. Syst. 53, 59–85. https://doi.org/10.1016/j.jmarsys.2004.05.027.

Vetter, L., Kozdon, R., Mora, C.I., Eggins, S.M., Valley, J.W., Hnisch, B., Spero, H.J., 2013. Micron-scale intrashell oxygen isotope variation in cultured planktic foraminifers. Geochim. Cosmochim. Acta 107, 267–278. https://doi.org/10.1016/j.gca.2012.12.046.

Walton, W.R., 1952. Techniques for recognition of living Foraminifera. Contr. Cushman Found. Foram. Res. 3, 56–60.

Wickham, H., 2009. ggplot2: Elegant Graphics for Data Analysis. Springer New York, New York. https://doi.org/10.1007/978-0-387-98141-3.

Wit, J.C., Reichart, G.J., Jung, S.J., Kroon, D., 2010. Approaches to unravel seasonality in sea surface temperatures using paired single-specimen foraminiferal $\delta^{18}O$ and Mg/Ca analyses. Paleoceanography 25, 1–15. https://doi.org/10.1029/2009PA001857.

Zervakis, V., Krasakopoulou, E., Georgopoulos, D., Souvermezoglou, E., 2003. Vertical diffusion and oxygen consumption during stagnation periods in the deep North Aegean. Deep. Res. Part I Oceanogr. Res. Pap. 50, 53–71. https://doi.org/10.1016/S0967-0637(02)00144-9.